uOttawa

L'Université canadienne
Canada's university

FACULTÉ DES ÉTUDES SUPÉRIEURES ET POSTOCTORALES

uOttawa

L'Université canadienne
Canada's university

FACULTY OF GRADUATE AND POSDOCTORAL STUDIES

Anastasia Vander Host
AUTEUR DE LA THÈSE / AUTHOR OF THESIS

M.Sc. (Earth Sciences)
GRADE / DEGREE

Department of Earth Sciences
FACULTÉ, ÉCOLE, DÉPARTEMENT / FACULTY, SCHOOL, DEPARTMENT

Recovery and Analysis of Historical Mine Data in a 3-D Environment: A Case Study – Heath Steele, Bathurst Mining Camp, Northern New Brunswick

TITRE DE LA THÈSE / TITLE OF THESIS

Dr. M. Hannington
DIRECTEUR (DIRECTRICE) DE LA THÈSE / THESIS SUPERVISOR

Dr. W. Goodfellow
CO-DIRECTEUR (CO-DIRECTRICE) DE LA THÈSE / THESIS CO-SUPERVISOR

EXAMINATEURS (EXAMINATRICES) DE LA THÈSE / THESIS EXAMINERS

Dr. B. Daneshfar

Dr. C. Samson

Dr. A. Desrochers

Gary W. Slater
Le Doyen de la Faculté des études supérieures et postdoctorales / Dean of the Faculty of Graduate and Postdoctoral Studies

Recovery and Analysis of Historical Mine Data in a 3-D Environment: A Case Study - Heath Steele, Bathurst Mining Camp, Northern New Brunswick

Anastasia Vander Most

Thesis submitted to the
Faculty of Graduate & Postdoctoral Studies
University of Ottawa
in partial fulfillment of the requirements for the
M.Sc. degree in the Earth Science

Ottawa-Carleton Geoscience Centre and
University of Ottawa
Ottawa, Canada

Thèse soumise à la
Faculté des études supérieures et postdoctorales
Université d'Ottawa
en vue de l'obtention de la maîtrise ès sciences
en sciences de la Terre

Centre géoscientifique d'Ottawa-Carleton
et
Université d'Ottawa
Ottawa, Canada

Your file Votre référence
ISBN: 978-0-494-49286-4
Our file Notre référence
ISBN: 978-0-494-49286-4

Table of Contents:

List of Tables:

List of Figures:

Abstract:

3-D geographic information systems (GIS) provides a powerful tool for visualizing and interpreting the subsurface distribution of geology and hydrothermal parameters that are important in exploring for deposits concealed at depth. For the purpose of this study, restoration of a historical mine data set was undertaken with the goal of migrating information from paper records to fully linked data sets suitable for interpretation in 3-D GIS. Heath Steele, in the Bathurst Mining Camp, northern New Brunswick, is one such deposit with historical records that include the distribution of ore-associated iron formation, massive sulfides and host rocks. Structural and stratigraphic interpretations from previous studies and exploration programs were incorporated in the model, along with fabric measurements, regional geology, drillcore logs and geophysical data. This study shows how revisiting historical mine data in a 3-D environment can generate new knowledge about an ore deposit and particularly the spatial context of hydrothermal features in a complexly deformed setting that may aid future exploration.

Résumé:

Les SIG tridimensionnels sont de puissants outils pour visualiser et interpréter la distribution sous-terraine de la géologie et les caractéristiques hydrothermales importantes pour l'exploration de dépôts minéralisés dissimulés en profondeur. Dans le cadre de ce projet, une réévaluation de données minières historiques a été entreprise avec l'objectif de migrer l'information disponible sur papier vers des données entièrement intégrées convenables pour l'interprétation dans un SIG tridimensionnel. La mine Heath Steele dans le camp minier de Bathurst est un de ces dépôts minéralisés avec des données historiques qui incluent la distribution des formations de fer associées à la minéralisation, des sulfures massifs et des roches encaissantes. Les interprétations structurales et stratigraphiques des études et campagnes d'exploration précédentes ont été incorporées au model avec les mesures structurales, la géologie régionale, les logs de forage et les données géophysiques. Cette étude montre qu'une réévaluation de données minières historiques dans un environnement SIG 3-D peu générer de nouvelles connaissances sur un dépôt minéralisé, et particulièrement sur la distribution spatiale des caractéristiques hydrothermales d'un environnement fortement déformé pouvant guider l'exploration future.

Acknowledgements:

This study was fully funded by the Geological Survey of Canada through the Targeted Geoscience Initiative (TGI) III - Deep Search headed by W.D. Goodfellow, and Appalachians project headed by N. Rogers. Field trip support was provided by New Brunswick Department of Natural Resources (DNR Minerals; Bathurst office) and led by C. van Staal. J. Walker. S. McCutcheon, J. Walker, R. Wilson, J. Langton and others at the New Brunswick Department of Natural Resources, Bathurst, New Brunswick, were valuable sources of information on the Heath Steele property and provided considerable assistance in the search for old thesis material and locating surviving drill core and records. N. Rogers of the Geological Survey of Canada, Ottawa, provided important insight on the complexity of the Bathurst Mining Camp. Funding from the TGI-III Appalachians project was provided for workshops and presentation at the Exploration 07 conference, held in Toronto, Canada.

Efforts by J. Peter in successfully locating old maps, cross sections and data are greatly appreciated along with his input at early planning meetings helping to define the scope and objectives of this project.

E. de Kemp has provided essential direction and guidance throughout the thesis in working with Gocad© and especially in trouble-shooting the critical and difficult process of migrating data into Gocad©. E. de Kemp and N. Megrez should also be recognized for their assistance with the calculation for the transformation from Mine Grid to UTM NAD83. I am also indebted to Mira Geoscience employees for help and support with Gocad© and its software intricacies, and to K. Sprague, formerly of NRCan, who was always willing to fix a bug in SPARSE© as soon as I found one.

To my supervisor at University of Ottawa, M. Hannington, I thank you for supporting me as a graduate student after I have been out of university for so long and providing valuable encouragement, edits, and improvements to this thesis and submissions for publications. To my co-supervisor at the Geological Survey of Canada, W. Goodfellow, I thank you for bring such an interesting project to my attention and providing me with the tools and people to accomplish such a challenging study. Improvements to this thesis were also made by your valuable edits.

Portions of this work were presented at the Society of Economic Geology (SEG) Bi-annual conference held in Keystone, CO (Vander Most and de Kemp, 2006) and at Exploration 07 held in Toronto, ON (Vander Most et al., 2007). Attendance at the SEG conference was partially funded by the SEG and TGI-3, and the Exploration 07 conference funded by the TGI III– Appalachians, which also funded field trips to Bathurst and Gocad© training at Mira Geoscience in Montreal. Research awards from SEG and CSEG (Canadian Society of Exploration Geophysics) are gratefully acknowledged.

1.0 Purpose and Scope of Study

1.1 Introduction

Mining and mineral exploration companies are increasingly looking at the extensions of known orebodies or the discovery of new orebodies at great depth within existing mining districts to replenish diminishing ore reserves. In most cases, the near surface mineral deposits have been identified by an arsenal of geophysical techniques, surface geochemical analyses and multi-scale geological mapping. Generally these targets are interpreted in 2-D (i.e., maps and sections) on the basis of limited subsets of data. Because of the complex three-dimensional nature of the orebodies, their host rocks and ore-related structures, exploration success in mature camps with potential for significant deeper deposits requires a more rigorous 3-D modelling approach of new and historical data.

Many large companies possess vast amounts of data that can be used to greater effect in developing exploration models for their camps or other camps with similar characteristics. Sillitoe and Thompson (2006) compiled data on precious and base metal deposits discoveries over the last 35 years and observed that the majority of the new discoveries are near existing mines or in established mining camps. Therefore, existing data sets in mature mining camps provide valuable information about future mining opportunities.

Exploration targets are generated through the application of expert knowledge and assessment of large volumes of data and models. Integrating geophysical, geochemical, mineralogical and petrological data in the same environment gives a user a more realistic understanding of their relationships and associations. One data layer by itself commonly does not provide enough information to define an exploration target, but incorporating multiple layers of information can help to identify or discredit anomalies as follow up targets.

This study explores how historical mine data, as well as earlier interpretations of the data (e.g., conceptual 2-D models) can be integrated into a single 3-D environment. The end product provides an important platform for testing, interrogating, assessing quality of interpretations, and a basis for future model construction of the deposits using all of the available mine data. Combining such data as regional trends (i.e., structural constraints on orebodies), orebody characteristics, and spatial relationships of orebody elements in a 3-D environment gives the user more visual context opportunities for the quantitative description of a target. The user can visualize data from different perspectives as plan views or cross sections, and can manipulate the type of data they want to see or use at one time. Queries, such as proximity to ore, intersections of faults and ore horizons, and geochemical spatial distribution further aid in interpretation, data integration and model construction. Three-dimensional modeling is a relatively new approach for incorporating different data layers in the same environment. Yet, 3-D modeling and methods for dealing with diverse sets of historical mine data are not well established.

To test various methods of integrating historical mining data, a 3-D model of the past-producing Heath Steele volcanogenic massive sulfide deposit in Bathurst Mining Camp of northern New Brunswick, Canada, was created. The Bathurst Mining Camp contains forty-five major deposits distributed along several discrete mineralized horizons (Fig.1). Lead, zinc and copper ores were mined from the Bathurst Mining Camp and are still being mined from the Brunswick #12 and Caribou, along with small quantities of Ag and Au. Heath Steele deposits were mined since the 1950s, but mining ceased in 1999. More than 50 years of data were amassed during the early exploration of the deposits, mine development, and subsequent mine-scale exploration. Industry, government and universities also have collected large amounts of data of different types from this area in an attempt to better understand the complex structural history and depositional environment of the deposit. Preliminary interpretations of these data by early workers (de Roo et al., 1991; McCutcheon, 1992; van Staal et al., 1992) indicates that there are multiple orebodies along the same horizon within the Heath Steele belt, but it has been difficult to follow the horizon due to the considerable structural complexities. This study investigates ways a 3-D GIS environment can assist in unravelling this ore horizon.

Previous 2-D models of the Heath Steele mine stratigraphy (Dechow, 1959; de Roo et al, 1990b; Moreton, 1994; Park, 1996) have been based on limited data sets in specific areas in the mine. A major challenge of this study was to place these 2-D interpretations into a three-dimensional context, thereby allowing these often conceptual models to be tested more rigorously. Incorporation of historical data and interpretations can help to assess model validity, make decisions about acquisition of new data, and possibly generate new alternative interpretations. In a 3-D digital environment, these decisions and interpretations can be made quickly and can include mapping of uncertainty, 3-D cross validation experiments, examination of spatial continuity, structural anisotropy, and more specific examination of exploration target vectors.

Since most companies will not drill to "discover" geology but only to differentiate between ore and waste, methods must also be developed to best fit the biased datasets that are amassed in the mine environment. On one hand, mine data is commonly restricted to ore zones (i.e., a spatially biased dataset), whereas conceptual 2-D models of the deposit geology typically extend beyond the ore zones. Integrating these two different data resolutions at Heath Steele was an important goal of this study. An outcome of the present study was the development of best practices for incorporating and using such data in a larger-scale, exploration-oriented 3-D model.

This study was initiated as part of the Deep Search project in the Geological Survey of Canada's "Targeted Geoscience Initiative 3" (TGI-3) Program. In 2005 the Government of Canada committed $25M over five years to TGI-3 to investigate areas of high base metal potential in Canada through innovative geoscience techniques. This study meets with committed outputs and outcomes by integrating existing industry and government data, improving methods for mapping, and creating a 3-D model of an established deposit. It also assists in increasing exploration discoveries by further understanding requirements for modelling of targeted areas and indicating where further exploration may indicate deeper deposits.

1.2 Benefits of GIS and a 3-D Environment

With most near surface deposits already discovered by conventional exploration methods, new and innovative techniques must be developed to explore for deeper ore deposits that are more difficult to find. Existing and closed mines have an abundance of data that help drive the knowledge of ore producing environments. This knowledge can then be applied to further extend ore zones in mineralized belts or to explore in areas where data is limited or non-existent. By making linkages to larger scales from mine scales, areas of low mineral potential (greenfields) may become prospective. Traditionally, deposit characteristics were defined by geostatistics, manual interrogation and interpretation of the data using maps and cross-sections. This type of data analysis was less effective investigating subsurface data distribution then it is now, which is now undertaken with a wide range of 2-D visualization and interpretation support tools. This is further enhanced by 3-D GIS, which interrogates and interprets data in its true spatial context of what the data represents: a 3-D ore deposit and its associated environment.

Geographic Information Systems (GIS) allows multiple data layers to be viewed together or separately, spatially queried, or defined using geostatistics. Objects in this environment are represented as map objects that can be manipulated and analysed individually or as groups (Bonham-Carter, 1994). Traditionally 2-D GIS treatment using software such as ArcMap© by Environmental Systems Research Institute (ESRI) has been applied by a variety of disciplines. Recent advances in GIS have led to 3-D methods that more realistically model spatial data. The petroleum industry has been using 3-D GIS for modeling reservoirs and future project development for quite some time, which is now being adapted by the mineral exploration community at large.

A widely used 3-D GIS program in mineral exploration is Gocad©, an Earth Decision product. This 3-D GIS software can be used to visualize, interpret and create a model from multiple data layers. This type of software was first used by the petroleum industry in the 1980s and is now being developed by the mineral industry and exploration companies for mine and near mine mineral exploration. Previous 3-D programs where developed exclusively for the mining and exploration industry but had limited applications for 3-D modeling or exploration beyond the mine site.

Procedures and workflows used by petroleum companies are for relatively simple structural settings of petroleum reservoirs from input data such as seismic surveys and electronic well logs, not 2-D map based objects. Similar procedures and workflows do not effectively work for mineral exploration in complexly deformed terrains, making it necessary to develop tools and modules for the more complex nature of mineral deposits. Whereas the petroleum industry tends to deal with simple structures and stratigraphy, the mineral industry deals with more complex folding, faulting, thrusting and variable fluid pathways when targeting large mineral deposits. Thus, application software designed for petroleum exploration to be utilized in the mine environment has been a challenge. This challenge is being met by agencies such as universities and government surveys, which are examining ways to handle the more complex nature of the deposits. For example, de Kemp and Sprague (2003) investigated and developed tools required in the 3-D environment to aid in structural interpretation in sparse settings.

Gocad© has the distinct advantage of handling both 3-D drillhole data and a variety of geophysical and geochemical data. Other software that utilizes drillcore data does not handle the same variety of data-types, nor does it have workflow modules that can be used to integrate 2-D and 3-D data in such complex structural environments or provide multiple viewing tools.

Geostatistics modules in Gocad© can be readily applied in the GIS environment to examine data values and their association with a certain location. Location can refer to a region (volume) or a point, which has an implied connection to the data. Modules within Gocad© such as kriging provide a probabilistic approach to understanding the spatial variability of data. Although these procedures are available in Gocad© and have been tested on the study data set, no results are included in this thesis as the study of variograms can itself be a research project on its own.

1.3 Purpose

Re-investigating historical data and interpretations that have contributed to understanding deposits in the past can be useful for future exploration of potential mineral-rich areas. Thus, three major questions are addressed in this study:

1) how can diverse sets of historical mine data, collected over the 50-year mine life, be most efficiently imported into the same georeferenced 3-D environment;

2) how can historical 2-D interpretations of the mine geology be fully integrated with the new digital mine database so that earlier models of the deposit can be tested and better constrained;

3) which feature(s) in the historical mine dataset can be most readily identified and traced in 3-D, thereby providing a possible guide to exploration in the mine environment.

Since data drives interpretations it is important to asses its quality and reference for the purpose of the project. Collection of the data can be a challenging task in itself, especially if the mine is now abandoned, making it difficult to gather data, projections, key legends, and past interpretations, and to locate experts familiar with the mine area. Therefore, a goal of this project is to establish a workflow for this type of 3-D geological integration to be used in other mines with large historical datasets.

The resulting integration of the Heath Steele deposits can be used to test a number of ideas arising from existing geophysical, structural and lithogeochemical studies. For example, the association between iron-rich sedimentary rocks and the underlying volcanogenic massive sulfide deposits has been well established throughout the camp (McCutcheon, 1992; Peter, 2003; Peter and Goodfellow, 1996; Peter and Goodfellow, 2003; Spry et al., 2000). However, the detailed 3-D structural relationships of this horizon and the ore hosting volcanic rocks are poorly understood in the Heath Steele belt. This study is the first of its kind to examine these relationships in the Heath Steele deposits in 3-D, and is the essential step in moving forward to a more rigorous interpretive stage that is such a big part of deeper, high risk exploration.

During the course of this study different modules in the 3-D and 2-D environment were developed or improved for 3-D model construction, such as SPARSE© in Gocad©, Dig-sym and Shape to Gocad© in ArcMap©. Workflow procedures in Gocad© were also tested to improve the application of this software by both specialist and non-specialists.

1.4 Discovery and Recent History of the Bathurst Mining Camp

The Bathurst Mining Camp has been prospected and studied since the 1800s. Work by prospectors, government agencies, industry and university researchers have contributed greatly to the current understanding of the Bathurst Mining Camp. Through mapping, geochemical and geophysical surveys, and drilling many occurrences of massive sulfide deposits have been found, 25 containing more than 1 million tonnes. McCutcheon et al. (2003) present a detailed camp history since the 1950s, which is briefly summarized below.

Prior to the Pb-Zn-Cu massive sulfide discoveries in the 1950s, the camp was well known for its Nepisiguit iron ore deposit. Early evidence of the massive sulfides was recognized in 1860s in copper-rich boulders. In the 1930s drilling identified the existence of massive sulfide bodies, but these did not become a specific target until the 1950s. In 1943, the province of New Brunswick contracted G.S. MacKenzie to report on the geology of the iron formation at Austin Brook (McCutcheon et al., 2003). The promising mineral potential south of the city of Bathurst prompted R. Skinner from the Geological Survey of

Canada to start mapping the area around Austin Brook in 1949. The first aeromagnetic surveys were flown as part of this mapping project in 1950 and 1951 (the first such surveys ever carried out in New Brunswick: McCutcheon et al., 1997). The complete history of the district before the 1950s can be found in MacKenzie's (1958) account of mining exploration in the Bathurst and Newcastle districts.

In 1952, the first major base metal sulfide deposit (Brunswick 6) was found by the M. J. Boylen Prospecting Group. Massive sulfides were intersected by follow up drilling on a ground electromagnetic anomaly. This began a staking rush and led to the establishment of the Bathurst Mining Camp. In 1954 ground geophysics was used to better define anomalies from the first airborne electromagnetic survey. This led to the discovery of the Heath Steele orebodies by the American Metal Company (AMCO). A significant number of massive sulfide occurrences were discovered in the second half of the 1950s through geophysical, geochemical, and prospecting techniques. In the years to follow further occurrences and economic deposits were identified through a better understanding of the stratigraphy and because of improved geophysical technology.

Discoveries in the past 10 years have not been as plentiful as in the 1950s (Fig.2), although in 1996, the Camel Back deposit was discovered by following up electromagnetic (EM) and magnetic anomalies that resulted from a survey undertaken by the Geological Survey of Canada during the Exploration Technology (ExTech) II Project. The findings of the ExTech II Project are published in Economic Geology Monograph 11 (ed. Goodfellow et al., 2003). One of the suggestions for further research put forward was to explore the "three-dimensional geometry of hydrothermal alteration zones associated with massive sulfide deposits and how can they be used as vectors to locate buried sulfide deposits in the Bathurst Mining Camp" (Goodfellow et al., 2003a).

1.5 History of the Heath Steele Mines

Ground geophysics was used to evaluate and better define many of the anomalies from the airborne electromagnetics surveys in the 1950s. This led to the discovery of the A zone on the Heath Steele property. Drill hole 54-2, in the A zone, intersected the first significant massive sulfides. Further drilling of other anomalies led to the discovery of four more massive sulfide zones; the B, C, D and E zone. All five deposits are believed to occur on the same massive sulfide horizon within the Nepisiguit Falls Formation at or near the contact between the felsic volcanic rocks (quartz feldspar porphyry) and iron-rich sedimentary rocks (sulfide bearing chloritic tuff). The A zone is west of the B zone, and more proximal to the North Little River Lake fold (Fig. 3). The B zone has two surface showings and was the largest of the deposits on the Heath Steele property. The C and D zones occur close to the A zone and could be considered as part of the same deposit, whereas the E zone is north of these zones but likely part of the B zone. Mining of copper-rich and lead-zinc ore from the A and B zones began as open pits. A summary of the past production from these zones is given in Table 1.

In February of 1957, the mill at Heath Steele began processing ore from the A and B open pits. In two years, 369,773 tonnes of 1.81% Pb, 5.14% Zn, 2.68% Cu and 105.0 g/t Ag were mined (Luff, 1995). The first shaft was sunk in the D zone in 1955 to a depth of 122 m. This zone was initially mined in 1957 and 1958 and shut down shortly afterwards along with the operations of the A and B zone. In 1962 mining resumed in the A and B zone and at the D zone in 1963. Also, in 1962 a second shaft was sunk to 116 m on the B zone mainly for exploration. A ramp was also driven in the B zone that was mined until 1970. No. 3 shaft was sunk on the B zone to a depth of 526 m in 1967 and in 1971 – 1972 the No. 4 shaft was sunk to 417 m on the C zone. A fifth and final shaft was sunk in 1975 -

1976 to a depth of 890m in the B zone. Intermittent mining took place until October of 1999 when the mine was permanently closed (Art Hamilton personal communication).

Table 1. Heath Steele mineral deposits displayed by company who discovered deposit, year of discovery and mineral resource estimates for tonnage (from Goodfellow and McCutcheon, 2003).

Deposit	Discovered by	Year	Mt	Pb (wt %)	Zn (wt %)	Cu (wt %)	Cu+ Pb +Zn (wt %)
Heath Steele ACD Zones	American Metal Co.	1954	6.11	1.48	5.51	0.84	7.83
Heath Steele B Zone	American Metal Co.	1954	69.9	0.89	2.69	0.98	4.56
Heath Steele C-North	Heath Steele Mines	1981	2.70	2.04	6.03	0.39	8.46
Heath Steele E Zone	American Metal Co.	1954	1.92	1.36	3.57	1.16	6.09
			Average for four zones listed	1.44	4.45	0.84	
			Cut off used in figure 26	2	5.5	0.5	

Mt = million tonnes of geologic reserves, does not include production from gossan or supergene zones.

2.0 Geological Context of the Bathurst Mining Camp and the Heath Steele Zone

2.1 Tectonic Setting

The Bathurst Mining Camp, located south of the city of Bathurst, encompasses a 70 km subcircular area in the northern Miramichi Highlands. The volcanic and sedimentary rocks of the region were deposited in the middle Ordovician. Four main groups of volcanic and sedimentary rocks comprising the bulk of the Bathurst Mining Camp rocks were deposited in the Tetagouche-Exploits back-arc basin during the middle Ordovician (van Staal, 1987, 1994a; van Staal et al., 1992). The back-arc basin developed to the east of the Popelogan Arc, which formed on the margin of the Ganderia continent (van Staal, 1994a; Williams, 1979). Westward migration of the Popelogan Arc led to extension, up-welling and thinning of the continental crust and eventual rifting and breaking away of four blocks with distinct stratigraphy (Rogers and van Staal, 2003; van Staal, 1987; van Staal et al., 2003a).

During the opening of Tetagouche-Exploits back-arc basin four major hydrothermal events occurred spanning 12 to 14 million years (Goodfellow and McCutcheon, 2003; van Staal et al., 2003a: Fig. 4). Each of these hydrothermal events is represented by a horizon where significant deposits have been found. The horizons are referred to as the Chester (478 Ma), Caribou (472-470 Ma), Brunswick (460-469 Ma) and Stratmat (465 Ma) (Goodfellow and McCutcheon, 2003; van Staal et al., 2003a). The Sheephouse Brook block hosts the Chester horizon, the California Lake block hosts the Caribou horizon, and the Tetagouche block hosts the Brunswick and Stratmat horizons (Goodfellow and McCutcheon, 2003; van Staal et al., 2003a). Heath Steele is located in the Brunswick horizon. The fourth block is the Fournier Block that does not have a distinct sulfide horizon nor any significant deposits. Figure 5 shows the current block distribution in the Bathurst Mining Camp.

The collision of the Popelogan Arc with Laurentia in the Caradoc (late Ordovician) led to the eventual closure of the back-arc basin (van Staal et al., 2003a). The division between the Dunnage and Gander zone (in New Brunswick) of the Appalachian Orogen is placed where Popelogan Arc and subsequent back-arc basin blocks accreted onto Laurentia (van Staal, 1994a; Williams, 1979). The continued westward migration, subduction and thrusting of the blocks onto Laurentia were episodes of the Taconian Orogeny which was responsible for the intense deformation of the ore-hosting package (see below).

Overprinting by intrusions and associated contact metamorphism indicate that subduction ended by the late Silurian. Two generations of plutonism are recognized in the Bathurst Mining Camp. The first was likely related to the late Ordovician subduction and final closure of the basin (metagranite on Fig. 1). The second and main stage of plutonism occurred in the late Silurian, likely during the Acadian Orogeny, creating Mount Elizabeth (southwest corner in camp) and the Pabineau Falls Granite (northeast corner of camp) (de Roo et al., 1990b; de Roo and van Staal, 1994; van Staal, 1994a).

2.2 Structural Context

Earlier workers mapping the camp noted its structurally complex nature. Skinner (1974) documented the steep dips and plunges of the units and postulated two main periods of folding. McBride (1976) documented at least four stages of deformation in his study of the Stratmat and Heath Steele Mines.

The multiple deformational events are seen at a regional and outcrop scale. Poor exposure, intensity of deformation and lack of and poorly preserved primary depositional structures add to the difficulty of unravelling the structural history. Several studies (de Roo et al., 1990b; McCutcheon et al., 1997; van Staal et al., 2003b) have attempted to correlate structural fabrics across the region by comparing their orientation, style, and overprinting relationships. Table 2 provides a summary of these events from different authors. The present distribution of rock units (and contained sulfide bodies) was mainly controlled by folds occurring in D_1 and to some extent D_2 events (de Roo et al., 1990b; McCutcheon et al., 1997; van Staal et al., 2003b). The first stage of deformation was related to thrusting of the arc and subsequent back-arc basin onto Laurentia in the late Ordovician. Two fold generations (F_1 and F_2) are thought to have developed during the progressive thrusting of D_1. Shear zones are also recognized across the camp. D_2 asymmetrical upright folds and local narrow shear zones create interference patterns between the F_1 and F_2 folds (van Staal et al., 2003a). The Moose Lake - Mountain Brook fault system, south of Heath Steele (Fig. 5), represents a D_2 shear zone. In the south of the Bathurst Mining Camp this shear zone separates the Sheephouse Brook Block from the California and Tetagouche Blocks. Analysis of folds and lineations by van Staal et al. (2003) determined that the California Lake Block was thrust over the Tetagouche Block (Fig. 4). Studies of local folding patterns at the Heath Steele mines indicate that the North Little River Lake fold (at the hinge of the Heath Steele mineralized zone; Fig. 3) is a F_2 fold (de Roo et al., 1990b).

Post D_2 deformation comprises mainly large-scale vertical folds and recumbent horizontal folds. de Roo et al. (1990) assigned the vertical folds (steep belts) to D_3 and the recumbent folds (flat belts) folds to D_4. Recent work from van Staal et al. (2003) indicates that the vertical and horizontal structures represent one generation of deformation (D_3 ; Table 2), with variable orientations related to zones of high versus low strain (final Taconia closure).

Table 2. Comparison of tectonic history of the Bathurst Mining Camp by de Roo (1990) and van Staal (1984 and 2003) (modified from de Roo et al., 1990).

Chronology	2003 Study (van Staal et al., 2003a)	1990 Study (de Roo et al., 1990b)		1984 Study (van Staal and Williams, 1984)
± 470 – 458 Ma (U/Pb)		Felsic plutonism (southwest of Heath Steele zone)		
Caradocian (late Ordovician) to Ludlovian (upper Silurian)	D_1 thrust, shear zones $F_{1a} + F_{1b}$ S_1 (some steep belts)	D_1 shear zone F_1 conical S_1 transposition foliation		D_1 thrusting $F_{1a} + F_{1b}$ S_1
Late Silurian to Early Devonian	D_2 shear zone F_2 upright folds S_2 steep to flat belts	D_2 shear zone (steep and flat belts) F_2 tight-isoclinal S_2 transposition foliation		D_2 steep belts F_2 S_2 steep
394 ± 1 Ma (U/Pb)		Felsic plutonism (Pabineau Granite)		
Devonian	$D_{3\ v+h}$ F_3 recumbent folds - steep belts Vertical folds -flat belts S_3 steep and flat belts	D_3	F_h recumbent folds (steep belts) S_h horizontal	D_5 Kinks and gentle recumbent folds F_5
		D_4	F_v upright folds (flat belts) S_v NW-striking	F_3 S_3 NE - striking
	D_4 regional dextral transpressive regime F_4 uplift S_4 steep belts (formation of Rocky Brook-Millstream fault system)	D_5	D_5 kinks F_5 upright folds of flat belts, plunging folds of steep belts S_5 NE-striking (formation of Tetagouche Antiform and Ninemile Synform)	D_4 kinks F_4

Chronology of events by van Staal (van Staal, 1987) and radiometric Zircon U/Pb age dates by Bevier (Bevier, 1988) as presented by de Roo et al. (1990)

The Tetagouche antiform and the Nine Mile synform are the dominant fold structures seen in the Bathurst Mining Camp (Fig. 5). These structures represent the youngest generation of regional deformation (de Roo et al., 1990b; van Staal et al., 2003a). Brittle-ductile splayed faulting of the Rocky Brook-Millstream faults accommodated the uplift of the northern portion of the Bathurst Mining Camp.

Most rocks in the Bathurst Mining Camp underwent high pressure – low temperature metamorphism. The Heath Steele area experienced high strain metamorphism, reaching its peak late in D_1 when the Heath Steele fold nappe was steepened. The pressure and temperature of metamorphism were estimated to be $365 \pm 20^{O}C$ and 5.5 ± 0.4 kbar (Currie et al., 2003).

2.3 Stratigraphic Context of the Deposits

There are four tectonic blocks recognized in the Bathurst Mining Camp, from oldest to youngest, Sheephouse Brook, California Lake, Tetagouche and Fournier Groups (Fig. 5). The Tetagouche and California Lake Groups host the majority of the massive sulfide deposits, and both are characterized by a bimodal sequence of felsic to mafic volcanic rocks. The California Lake Group contains approximately equal amounts of felsic and mafic volcanic rocks, possibly representing a marginal basin underlain by oceanic crust and remnant continental crust. Felsic volcanic rocks dominate the Tetagouche Group, which is thought to have formed in a different extensional basin but also underlain by continental crust (Goodfellow et al., 2003b).

Preserved stratigraphic sequences indicate variable redox conditions, volcanic activity, and ocean depth. Bottom water alternated from anoxic to well oxygenated (Goodfellow and McCutcheon, 2003). Deposition of the Arenigian black shale of the

Knights Brook and Patrick Brook formations (lowest formation of the three older Groups) and the felsic volcanic and sedimentary rocks of the Nepisiguit Falls (Tetagouche Group) and Spruce Lake Formations (California Lake Group) occurred in an anoxic environment. This is thought to correspond to a global anoxic event in the Middle Ordovician, represented by widespread global black shales (Authur and Sageman, 1994). In the Llanvirian, deposition of maroon shales and cherts occurred in a well-oxygenated environment of the Little River (Tetagouche Group) and Boucher Brook Formations (California Lake Group) (Fig. 6).

Formation of most of the massive sulfide deposits predated the Llanvirian shales and cherts (Goodfellow, 2002). The Flat Landing Brook Formation in the Tetagouche Group marks a transition from a shallow marine to subaerial volcanic environment and back to marine conditions. In the Caradocian, the basins became deeper and returned to anoxic conditions, possibly due to subsidence from continued rifting in the basin (Goodfellow et al., 2003c). Of the four groups, the bimodal Tetagouche Group represents the most important ore-hosting stratigraphy, including the Brunswick horizon. Twenty-three of the forty-five major deposits in the Bathurst Mining Camp are in or near the Brunswick horizon consisting of altered mudstone and/or volcaniclastic rocks.

Other deposits, such as those in the Heath Steele belt occur in the Nepisiguit Falls formation of the Tetagouche Group (Fig. 4). The quartz ± feldspar porphyry of the Nepisiguit Falls Formation either pre-dates or post-dates the deposits, and its age has been constrained to ca. 470 Ma by several U-Pb isotope ages (Goodfellow and McCutcheon, 2003).

2.4 Massive Sulfide Deposits of the Bathurst Mining Camp

All of the massive sulfide deposits of the Bathurst Mining Camp formed by hydrothermal fluids venting at or near the paleoseafloor (McCutcheon 1992). Following deposition, the orebodies underwent polyphase deformation making it difficult to determine the original depositional setting. The massive sulfide bodies are commonly located in the hinges of D_1 folds and in local narrow shear zones (van Staal et al., 2003a). Many of the orebodies have been thickened by interference of F_1 and F_2 folds (de Roo and van Staal, 2003).

The deposits are classified based on composition as Zn-Pb-Cu type (Franklin et al., 1981) and are of bimodal siliciclastic type based on host-rock lithologies, which include roughly similar portions of volcanic and siliciclastic rocks (felsic volcanic rocks being dominant; Barrie and Hannington, 1999). Deposits of this type typically are larger than other volcanogenic massive sulfide deposits, with higher Ag and lower Cu (Barrie and Hannington 1999; Franklin et al., 2005).

Cumulative, polyphase deformation in the Bathurst Mining Camp masks an obvious heat source (such as a large subvolcanic intrusive body, that could have driven the convection of seawater and hydrothermal fluid), or clearly defined focused discharge zones for the fluids (such as synvolcanic faults and fissures). However, distal products of hydrothermal discharge (i.e., iron formations) are well developed in the district (Franklin et al., 2005; Peter, 2003) and are a major target for exploration.

The deposits range in shape from mounds to tabular bodies and, where proximal to vent complexes, show evidence of zoning and veining (Brunswick 12, 6, and Heath Steele B-zone deposits:(McCutcheon, 1992; McCutcheon et al., 1993). Other deposits such as

Canoe Landing Lake are more distal and lack a vent complex or zoning (Goodfellow, 2002).

The main ore horizons developed below a deep anoxic water column, indicated by the lack of bioturbidation (no reworking of sediments by organisms likely due to lack of organisms because of the reduced oxygen marine environment) and presence of black shales (Goodfellow and McCutcheon, 2003). In this environment, if the bottom currents were low as expected in a deep marine basin, a hydrothermal plume will not travel far and the fallout will be proximal to the vent. Work by Peter and Goodfellow (2003) showed that vent fluids formed buoyant plumes from which sulfides precipitated proximal to the vent. Distal zoning does occur, indicating the sulfides did not always precipitate as soon as the fluids vented onto the seafloor. This can be seen in metal zonation (Fig. 7) and in the nature of the ore horizon. Distal sulfide zones consist of fine layering of the sulfides and sediments, whereas the proximal zones are thicker and locally brecciated massive sulfide mounds.

A component of the metasedimentary rocks of the Nepisiguit Falls Formation of the Heath Steele belt (Figs. 4 and 8) is a greenish gray to dark gray siltstone layer (referred to as the chloritic tuff) which was deposited along with a laterally extensive iron formation. Three facies have been recognized in the iron formation: oxide, carbonate and silicate, reflecting differences in the depositional environment or in the composition of the venting fluids (see below). The ore deposits typically occur at or below these units (McCutcheon et al., 1993; Peter, 2003).

2.5 Massive Sulfide and Iron Formation Occurrence in the Heath Steele Zone

Five main ore zones are found at or near the surface on the eastern limb of the North Little River Lake Fold on the Heath Steele property (Figs. 3 and 8b). They consist of massive, fine-grained Pb and Zn sulfides with moderate but higher amounts of Cu than in most other deposits in Bathurst Mining Camp (Table 1). Polyphase folding of the ore horizon strongly influenced the shape and geometric distribution of the ore lenses and the associated iron formation; with the main orebodies occurring near fold hinges and on the limbs at the contact between volcaniclastic sedimentary rocks and a hanging-wall of quartz feldspar porphyry of the Nepisiguit Falls Formation (Fig. 8b: McCutcheon, 1990; van Staal and Luff, 1990). Iron formation occurs along strike from the deposits stratigraphically higher then the massive sulfides in the Nepisiguit Falls Formation. The spatial and temporal association of the iron formation with the massive sulfide is well documented (de Roo and van Staal, 2003; Goodfellow and McCutcheon, 2003; Peter, 2003; Peter et al., 2003; van Staal et al., 2003a). The carbonate iron formation facies interpretation is that it was deposited in deeper water relative to the oxide facies, in a mildly reducing environment and is composed of mostly siderite. The oxide iron formation facies was deposited in shallower, moderately oxygenated water and is dominated by magnetite. The silicate iron formation facies is more distal and is now composed of chlorite schist (Peter et al., 2003). Interlamination of minerals of the different facies (magnetite, carbonate, quartz and chlorite) indicate that the paleoredox conditions may not have been the main factor in controlling the formation of different iron formation facies and may in fact reflect a chemical changes in the composition of hydrothermal fluids (Peter and Goodfellow, 1996; Peter et al., 2003).

Deformation of the ore horizon resulted in complex relationships with the other lithological units and possible repetition of stratigraphic units. At a regional scale, the Heath Steele "zone" seems to be controlled by a regional D_1/D_2 structure (North Little River Lake fold: Fig.3). However, cross sections drawn from drillcore data by Noranda geologists indicate that the folding and thrusting at much smaller scale controls the final distribution of ore.

A simplified stratigraphic sequence of the Heath Steele zone is composed of footwall (chloritic tuff), massive sulfide with the associated late stage iron formation, and the uppermost unit, the hanging wall (quartz ± feldspar porphyry: Fig. 8a). These terms are adapted from mine terms used by previous workers. Table 3 lists the different terms used by mine geologists for host rock and is compared to terms used by Moreton (1994) in his thesis work. For the purpose of this study the column in the middle indicates descriptive terminology used to define the hanging wall and footwall units.

Table 3: Comparison of mine terminology for Heath Steele stratigraphy and terminology proposed by Moreton (1994) (modified from Moreton, 1994).

Mine Terminology	This Study	Moreton Thesis
Mafic volcanics Massive rhyolite Acid volcanic rocks Quartz feldspar crystal tuff Quartz crystal tuff	Hanging Wall (Quartz feldspar porphyry)	Felsic metavolcanic rocks
Iron Formation Massive Sulfides	Iron Formation Massive Sulfide	Iron Formation Massive Sulfide
Clastic sedimentary rocks Quartz crystal tuff Clastic sedimentary rocks Quartz crystal tuff Clastic sedimentary rocks Quartz feldspar crystal tuff	Foot Wall (Chloritic Tuff)	Footwall metasedimentrary rocks Massive felsite unit

Magnetite, siderite and stilpnomelane in the iron formation have a proximal association with massive sulfides making them effective indicators of ore along the Heath Steele horizons on a more local scale (Peter and Goodfellow, 2003). However, the iron formation unit is not a continuous unit along strike, nor does it have a consistent thickness, making it difficult to trace from zone to zone, from deposit to deposit and within a deposit. Chloritization occurs dominantly in the footwall sedimentary rocks throughout most of the deposit and its association with the massive sulfides is also apparent on a regional scale.

3.0 Data Integration

Much of the data used in this project was from the pre-digital era and was not fully archived, documented or properly preserved. Compiling this historical dataset into a digital GIS format and creating and documenting lost transformation calculations was a major part of the study and has significantly improved the quality of the data for future use. Integrating all the data into common coordinates required the use of special conversion software, "rubber sheeting" techniques, and mathematical transformations. In addition, it was necessary to re-classify lithology codes into a common modern form and to maintain consistent codes between the surface and subsurface drillcore.

3.1 Workflow

When creating a model from historical data, time must be allocated for a thorough investigation of the availability and quality of the data, its initial characterization, conversion of coordinates, and identification of thematic consistencies among interpretations of different workers. This can be the most daunting and time-consuming step in the construction of the model, but readily available 2-D GIS programs, such as ArcMap©, and specialized modules allow data to be compiled, ranked and registered in 2-D before migrating to the more complex 3-D environment. Spreadsheets and databases accessible through the 2-D and 3-D environments can also be used to re-class and organize data used for interpretations and model building. Throughout the construction of the model, data and interpretation must be kept separate in order to judge the uncertainty of interpreted objects within the model.

A workflow can be described as a series of repeatable steps designed to reach an objective/outcome. Initially, different paths have to be investigated to determine how best to achieve the defined objective. Through iterative testing of the various integration pathways a best path that is repeatable and efficient tends to emerge. This path becomes the skeleton of a workflow that can become the basis for software interface development.

A simple workflow was investigated for this study and is described below and is summarized in Fig. 9. This workflow suggested for integration of different data types into a 3-D environment can be used for other projects, not only for analysis of mature or historical data sets, but also at the planning and implementation stage of new exploration programs.

3.2 Types, Sources and Spatial Characterization of Historical Mine Data

From the first airborne electromagnetic survey in 1953 to closure of the mine in 1999, various types of data have been collected at Heath Steele. Mapping of outcrop exposures, structural fabric measurements, lithogeochemical analyses, geophysical surveys, till sampling, mineralogical studies, and isotope dating have been carried out. Various geological interpretations, correlating geological units between areas and mapped outcrop, and reconstructions of the deformation history also were prepared, but these have been based on limited subsets of the available geological information. Over 50 years, these interpretations also have been affected by a wide range of emerging geological concepts (McCutcheon et al., 2003).

The 3-D dataset of Heath Steele created in this study provides a framework to test many of the existing geological interpretations of the deposit using a variety of data layers that have not previously been integrated in a GIS or 3-D environment. Data that was incorporated in the 3-D environment included all drillcore data (5997 drill holes with lithology and assays - statistics of the drillcore data in Appendix A), digital elevation data, structural geology and geophysical data (Table 4). Interpretive cross sections and regional geology maps also were included. Each of the input data types is described in more detail below.

The drillcore data are the only accurately surveyed information of the deposit at depth. The most up-to-date format available was a digital database in Gemcom (by the company called Gemcom). Gemcom is mining software designed for grade and tonnage analysis, and to visualize geological data such as drillhole logs and sections in 3-D space. The drillcore data is stored in a Microsoft Access database.

Core logging was originally done by hand beginning in 1954, and included written lithological descriptions, structures (e.g., broken core) and estimated sulfide content. Assay values were incorporated during the construction of the Gemcom database, which was only completed just before the mine office closed in 1999. For the 3-D modelling, drill-collar locations, surveyed drillcore pathways, rock codes and rock assay values were extracted from the database. The available data was in Heath Steele mine grid coordinates (feet) that had to be converted to New Brunswick Grid coordinates, then to UTM coordinates (meters). The transformations between these coordinates developed for this study is explained further in the next section.

2-D sections drawn perpendicular to the geology surface were created from the drillcore data by Noranda mine geologists to identify and model the stratigraphy and structure. The drillcore data were projected from off-section onto a common section by hand, at intervals of 100 m, using an influence of approximately +/- 25 m from the section.

Table 4. Summary of data that was used in Gocad© outlining the year data was published/originated, source of the data, original format and coordinates. Further details of how the data was converted from its original coordinates to NAD83 UTM zone19N is explained in the text.

Year Published/Created	Data	Author/Source	Format of Data	Original Coordinates
2001	Regional Geology	van Staal et. al., 2001	Hard copy and digital Arcmap© files	NAD 27 UTM zone 19 and 20 N
1954 to 1981	Drillcore logs	Heath Steele Mines	Hard copy converted to digital Gemcom database	Mine engineering grid
1987 – 1991	Drillcore logs	Noranda	Hard copy converted to digital Gemcom database	Mine engineering grid
1992	Structural measurements	Reg Wilson, 1992	Hard copy maps, Caris	ATS 1977
1998	Structural measurements	de Roo et al., 1998	Harp copy journal figure	Mine engineering grid
	Cross Sections	Noranda	Hard copy and scanned digital images	Mine engineering grid
	Digital Elevation Model (DEM)	Noranda	Digital X,Y, Z point file	NAD83 UTM zone 19N
	Airborne Total Field Magnetics	Noranda	Digital X,Y,value point data	NAD83 UTM zone19N
2001	Hydrothermal sedimentary index data	Peter and Goodfellow, 2003	Digital Excel spreadsheet	NAD 27 UTM zone 19/20 N

Originally these were constructed on large mylar sheets, which are retained by the New Brunswick Department of Natural Resources office in Bathurst, New Brunswick. Forty cross sections were available as digital or hard copy images previously compiled by mine geologists. The hard copy images were scanned and incorporated along with the original digital images into the 3-D environment.

Digital elevation models (DEM, UTM NAD83 zone19N) of the mine area were available from Department of Natural Resources of New Brunswick and Noranda (now Xstrata Zinc). There were only minor differences in the elevation values, but the more recent DEM file from a Noranda airborne survey was used (Fig. 10). The present day elevations are different, as the property has been re-contoured to control water flow since the closure of the mine in 1999.

A new regional geology map (1:100,000) of the Bathurst Mining Camp produced as part of the ExTech II project and published in 2003 (available digitally on a CD as part of Economic Geology Monograph 11) was used to constrain the surface geology. Much of the interpretation used in the construction of the map was based on geophysical data, structural information and limited outcrop exposure (van Staal et al., 2003b). It was used as a guide to integrate drillcore data with the different lithological formations, regional faults, thrusts and folding.

In the Heath Steele mine area many fabric measurements have been taken to determine the possible structural controls on the location of the massive sulfide deposits. Mine geologists and researchers were able to take measurements at outcrops, in the open pits and in trenches when the mine was open (de Roo et al., 1990a; de Roo et al., 1990b; Moreton, 1994; van Staal, 1987; van Staal, 1994b; van Staal et al., 1992; Wilson, 1992). No original datasets or field notes were recoverable for this study, but structural measurements were compiled from hard copy published maps that were converted to digital images, rectified and digitized.

Multiple airborne and ground geophysical surveys have been conducted over the Heath Steele mine area. For this study, an airborne magnetic dataset was included as an example of integrating geophysical measurements into the 3-D model to identify the magnetic anomalies that are of potential interest for further follow-up exploration. The magnetic data was obtained by Noranda (through a joint venture called SLAM) and processed by their geophysicists, and the results where provided as a point file over the Heath Steele property.

Collecting and interrogating data is an important step in which sufficient time and effort must be allocated. Part of this process is understanding the level of uncertainty and error in the data. The uncertainty in the data used in this study is shown in table 5, along with its impact, the estimated error and the confidence given to the estimation of that error.

3.3 Transformations, Reconstruction and Harmonizing of the Mine Database

Because this study focuses mainly on the use of historical or mature mine exploration data, an effort was made to validate the spatial accuracy of the information by integrating all of the data into the same coordinate system. This required transformations of whole data sets and was a major challenge in the preparation of data for the 3-D model. All data brought into the 3-D model from a variety of coordinate systems was registered in UTM Nad83 zone 19N (Table 4).

All hard copy maps and cross sections of Heath Steele and drillcore data provided were in Heath Steele Mine Grid coordinates (feet). None of the drillcore data had UTM NAD83 coordinates in the database, and the transformation source to convert mine

Table 5: Uncertainty and estimated error of input data used for this study.

Data used for Interpretation	Source of Uncertainty	Impact	Max/Min Estimated Error	Confidence of Error Estimation *
Rock code intervals from CSV	Attention to original logging Conversion of paper to digital	Thickness of rock units	+/- 50 cm	75%
Rock code naming	Original logging - different loggers Change of codes over time (see Table 3) Conversion of paper logs to digital Convert from multi rock code to simple rock naming convention Interpolating blank intervals	Correct and accurate rock identification	70% accurate	60%
Assay intervals from CSV	Original logging – different loggers Conversion of paper to digital	Thickness of interval with specified Cu, Pb, and Zn values	+/- 50 cm	70%
Historical cross sections	Original construction projection parameters unknown Lithology characteristics not the same as drillcore data	Continuation of lithological units from one cross section to next	Projection +/- 20 ft	60 %
			Interpretation accuracy 60%	70%
Digital elevation model	Airborne altimeter data from old survey, may be different then what topography looks like today.	Elevation applied to other data for topography	+/- 10 cm	80%
Digital surface geology	Map interpretation from some outcrop exposure and rest from geophysical surveys	Contact of units Surface showing of geology	70% accurate	65%

* estimated error was a best guess, thus this is the confidence in the best guess where 100% is very confident and 0% is no confidence.

coordinates was unknown. It is common practise to create a local mine grid that has its orientation along and across the structural grain. There was no requirement to integrate information from separate mines to a common regional reference as exploration is focused locally. Thus a major challenge of the study was to determine the transformation from the local mine grid coordinates to an accepted national standard to accurately locate both the surface and subsurface drillcore data.

The transformation calculation was achieved by using the origin point of the Mine Grid in the New Brunswick Stereographic projection coordinates and two monuments that have been measured and documented in both coordinate systems. The original origin point coordinates of the mine grid have been lost, but was recovered using an old autocad drawing file in Mine Grid coordinates and an orthophoto in New Brunswick coordinates. Common roads and features were 'rubber sheeted' (matched) in ArcMap© by overlaying the autocad file on the orthophoto (Fig. 11). A similar approach was used by Kirkham et al. (2006) to determine a transformation conversion on a 3-D study of the Con and Giant gold deposits in Yellowknife. The Heath Steele Mine autocad file was provided by Art Hamilton, a past employee of Heath Steele Mines; the orthophoto was supplied by Service New Brunswick. Table 5 shows the points used from the local Mine Grid coordinates and the corresponding New Brunswick stereographic projection. The calculated linear transformation equations now available to convert local Mine Grid coordinates to New Brunswick NAD83 Double Stereographic coordinates are:

$$x_{NB} = 1.0044 \cdot x_{MG} - 0.01155 \cdot y_{MG} + 2522608$$
$$y_{NB} = 0.000576 \cdot x_{MG} + 1.0062 \cdot y_{MG} + 7581916$$

Appendix B shows the calculations used to derive the equations.

Table 6. Input points in both Mine Grid and New Brunswick coordinates used to determine the transformation equation. The local mine grid coordinates are in feet and must be converted to meters. The final equation to compute the x and y values from local Mine Grid coordinates to New Brunswick Double Stereographic coordinates is shown above (input transformation equation and math provided by N. Megrez of NRCan, Ottawa office).

Point ID	Local Mine Grid Coordinates (feet)		New Brunswick NAD83 Double Stereographic Coordinates (meters)	
	Easting	Northing	Easting	Northing
Origin reference	0.0	0.0	2522608.00	7581916.00
Monument NB27920	34156.6	18354.2	2533001.01	7587551.08
Monument NB26976	39400.4	22127.0	2534593.23	7588709.09

The depths of the drill holes were in feet, thus a simple conversion factor (1 foot = 0.3048 meters) was applied to convert meters down hole. In addition to the drill collar locations, the drillcore survey files, which provide the dip and azimuth down hole along the drill pathway were required. The 'DISTANCE' intervals in the drillcore survey file and the 'FROM" and 'TO' intervals in the rock code (geology) and assay (property) files, were converted from feet to meters.

The rock codes are a database describing the lithology observed in the drillcore by a numerical value. A legend of old rock codes helped to decipher the database. The codes themselves are a combination of lithology, alteration and fractures (broken core). To separate the different parts of this information, a unique lithology identifier was manually extracted from each entry of all 5997 core logs. In the final 3-D dataset all the intervals were assigned a lithological code to make a continuous core. Other parameters (e.g., alteration and fractures) in the written logs did not have to be continuous. Alteration data was not added to the presented dataset, but can be readily incorporated as an additional property in the model. In the case where no lithological code was given, the rock code interval immediately above was duplicated, basically using a nearest neighbour interpolation to have a continuous core record. The outcome was seven different rock types represented by a unique number (Table 6). Over the years of logging core the terminology changed and different companies/people logged the core, raising some question about the reliability and consistency in application of the rock codes. Certain lithologies (e.g., massive sulfides) were more faithfully recorded than others. The resulting digital database provided by this study is based on an interpretation of the written rock descriptions that had been converted to a digital code. This interpretation does introduce uncertainty in the rock code dataset and was accepted at the time of this study. A suggested method to decrease this uncertainty would be to have one person re-interpret all the original drillcore logs and develop a standard rock code database, a very time consuming process, thus this step not taken at this time.

Table 7. Rock code lithological codes used to bring in drillcore data into Gocad©.

Numerical Code	Rock Code
0	Casing
1	Chloritic Tuff
2	Tuff
3	Massive Sulfide
35	Iron Formation
4	Quartz/Feldspar Porphyry
5	Dyke
6	Felsic Volcanics
7	Mafic Volcanics

Historic cross sections which were interpreted from the drillcore data provide good visualization of the stratigraphy. Forty cross-sections were available (scanned or in hard copy) scaled down from the original mylar drawings. These were converted to JPG files to reduce the file size. Coordinates on the cross-sections are mine grid, where depth is given in a positive up direction with surface elevation at approximately 8800 ft (it is a common mining convention for depth to always be positive and to add a value to compensate negative deviation numbers). The scanned cross-sections were registered to the proper projection only after they were brought into the 3-D environment (discussed in the next section).

Limited structural data were obtained from hard copy published maps. One set of data was from R. A. Wilson (Geology of Heath Steele – Halfmile Lakes Area; Northumberland County, New Brunswick, 1993). This included a series of maps at a scale of 1:20 000, four of them covering the Heath Steele area. These four maps were scanned, converted to digital images, loaded into ArcMap© and registered in their published projection of Atlantic Transform System, 1977 (ATS77). Because two UTM central meridians cut New Brunswick, this province has adapted to its own projection (New Brunswick NAD83 Double Stereographic projection) making it easier for province wide mapping on one map sheet instead of two. Both of these projections are accepted in GIS software and allow ATS77 to be transformed to UTM coordinates. Using a plug-in available in ArcMap© (Dig-Sym) the structural measurements on the digitally rectified map were hand-digitized using the right-hand rule. This utility captures the strike from the mouse motion used to digitize the feature on the map and the dip was input numerically from the keyboard. The unique ID, type of measurement, strike trend, and dip was captured in a point feature attribute table.

The other data set used for structural information was a map published by de Roo et al. (1990). Only the hard copy was available, and it was scanned and saved as a digital image. Mine grid coordinates on the map provided points for registration into UTM NAD83 Zone 19N in ArcMap©. The map was rectified in ArcMap© and the structural measurements digitized using the Dig Sym plug-in. This map differentiated the deformational generations (D_1, D_2, etc.), which were included in the attribute table.

The regional map available in digital form (UTM NAD27) was brought into ArcMap© and converted to UTM NAD83 zone 19N through an ArcMap© projection (the proper digital conversion file can be downloaded from the internet, as it is not a standard file with installation of ArcMap©). The faults and thrusts from this map were also captured and projected to UTM NAD83 zone 19N, along with roads and waterways.

The residual airborne magnetic data was available digitally and in UTM NAD83 zone 19N. Noranda carried out the original quality inspection and processing of the data. The input data consists of X and Y positions and magnetic point data with spacing of 50 m along lines and 200 m between lines (flown 160 m above the terrain). No preparation was required to bring these data into the 3-D environment.

3.4 *Integrating and Registering Multiple Data Sets into a 3-D Environment*

The Gocad© software was chosen as the 3-D environment to integrate the Heath Steele data for its capability to support 3-D vector and raster data and the ability to conduct spatial queries. To incorporate data into the 3-D environment Gocad© input formats and input wizards (i.e. import drillhole wizards) were used and in some cases objects could be loaded directly by converting ArcMap© shape files to Gocad© objects through a plug-in in ArcMap©. Integration of the Heath Steele data into a 3-D environment, such as the drill pathway, lithology codes and geophysics, does not tell us anything new about the data, but does give us a new perspective to view the data and the ability to create a model.

All the surface and subsurface drillcore data, converted to UTM NAD83 zone 19N and meter units, were parsed into separate CSV files for location, survey drillhole information, geology and other properties, which were then imported into Gocad© using a drillhole wizard. The required two files for the drillhole wizard are the header and survey files. The header file requires a unique ID, X, Y, and Z of each collar location and total length of core. The survey file contains the unique ID, DISTANCE intervals, Dip and Azimuth of the drill path. With these two files the drill pathway can be displayed in the correct georeferenced space (e.g., Fig. 12). Properties can be added to the drillcore path, such as the rock code lithology, assay values and any other rock property that can be connected to a drillcore interval. Rock properties, such as geology, can be input as a geology file and represented as zones or top/bottom markers on the survey path. Other rock properties, such as assay values, can be input as a property file that then becomes a log file in the model. These files contain an ID, FROM and TO intervals and numerical TYPE data. In the property file, multiple TYPEs of data (such as whole-rock geochemistry) can be input in one CSV file (see Appendix C for sample CSV files for drillcore input data). Once integrated with the drillcore pathway, these properties can be visualized in 3-D along the pathways (Fig. 13). The lithology is converted to a curve (polyline) object to more efficiently handle and visualize the rock codes. The Cu, Pb, and Zn assay logs are also converted to three different curve objects. Converting to curve objects from the original drillcore CSV file requires a sample input parameter from the program, thus it is necessary to choose a sample rate that ensures the data is represented accurately. A 0.30 m interval for the assay data was used to try and capture as much data as possible without causing the files to be too large for the working environment (see Appendix A for assay interval sizes). By converting the properties from the drillcore data to curves they can be treated as objects, which can then be queried to create regions of specific targeted data.

The cross sections were more challenging to reference in the Gocad© environment because they were only available in mine coordinates. The digital images were imported as 2-D voxets (images). To reference the cross sections, grid lines along which the cross sections were drawn from, were converted to UTM NAD83 zone19N. The depth displayed on the cross sections also had to be converted. A correction of the mine elevations to sea level (-7855.3 feet) was found in a thesis by Dechow (1959). Feet units were converted to meters to keep all the data consistent. Once all the cross sections were referenced in Gocad©, their positions were visually inspected by comparing them to a mine grid showing the location of the cross sections and the DEM (Fig. 14). The DEM was imported as a XYZ column file and used to interpret a surface representing the BMC area.

The structural data digitized and referenced in ArcMap© was loaded as point objects in the 3-D environment (Fig. 15). A plug-in in ArcMap© called 'shape 2 gocad' converts shape files into Gocad© objects and copies selected attributes along with the X, Y and Z positions. As long as the shape file is in the correct projection, it is a simple procedure to load into a Gocad© project as points, curves (polylines) or surface (filled polygon) objects. The structural data differentiated by generations (D_1, D_2, etc.) was given an additional attribute to define its generation, so that a region can be created to capture only those measurements associated with a particular deformation event. The structural data can be classified as structural measurements in Gocad© by the addition of strike and dip properties, which are then used to define dip markers in the Gocad© environment (Fig. 15b).

The compiled regional geology, including faults, thrust faults, roads and waterways was brought into Gocad© as curve objects. These data layers were converted to Gocad© objects in ArcMap© with the plug-in 'shape 2 gocad'. The geology surface (filled polygons) was loaded as one object. This object is more useful split up by individual lithologies. Querying specific lithologies and transferring them to individual surface object files, allows each unit to be displayed separately. The Z (elevation) value for the geology surface objects was transferred from the DEM (mentioned above) to the lithological unit (Fig. 16)

The airborne residual magnetic intensity data were imported from an X, Y, Z, point object file. These point objects were then used to create a pseudo surface through Discrete Surface Interpretation (DSI) in the Gocad© environment (Fig. 17). The residual magnetic intensity can also be viewed as pseudo topography to easily visualize the amplitude difference.

4.0 Modelling of the Heath Steele Data

In this study, the iron formation at Heath Steele was chosen as a key feature to highlight, owing to its close association with the massive sulfides in the mine and beyond. It was deposited after the major episodes of hydrothermal venting responsible for the formation of the massive sulfides (Peter and Goodfellow, 1996; Peter and Goodfellow, 2003). It was thought to be more continuous and tabular in shape than the massive sulfide bodies. In addition to being more laterally extensive than the massive sulfide deposits, the iron formation may have behaved more coherently than the pod-like massive sulfide deposits and their associated stockwork mineralization during deformation flow and transposition. Previous stratigraphic models suggest that the iron formation has a spatial relationship to the massive sulfides such that it is commonly located stratigraphically above or adjacent to the massive sulfides (de Roo and van Staal, 2003; Goodfellow and McCutcheon, 2003; Peter, 2003; Peter et al., 2003; van Staal et al., 2003a). In this study, attention was given to investigate this relationship through visual inspection in a 3-D environment of the iron formation and massive sulfide as logged in the drillcore data. Also of interest was the quartz feldspar contact horizon which is of importance as it may represent a volcanic – volcanic clastic transition zone. These zones are important for understanding massive sulfide deposit environments as they signify hiatus versus volcanism.

4.1 Modelling of the Iron Formation, Massive Sulfides, Hanging-wall, and Footwall Contacts at Heath Steele

Various interpretation methods were utilized to delineate the iron formation and the massive sulfide orebodies. An advanced tool in the Gocad© environment (SPARSE©)

allows the user to create sectional planes onto which any combination of objects can be projected (Sprague and de Kemp, 2005). The sectional planes can also be used as a surface for digitizing user interpretations. To orient the sectional planes, a voxet (cage) is created to encompass the selected data for digitizing (Fig. 18). Optimally the principle axis should follow the strike of the object of interest (U). In this study the principle axis of the voxet was the general strike trend of the iron formation and massive sulfide horizon. Optimizing this trend will allow perpendicular sections to the structural grain of the area of interest. Four voxets were created, one each for the ACD zone, B zone, E zone and the West ACD zone (Fig. 19). The voxet volume can be divided into user specified cell sizes by dividing the three axis (U, V, and W) by a selected number of intervals. It is important to represent the axis of the greatest variability with the largest number of divisions. Once an optimal voxet is created for orientation and cell division the 'Sparse' module can generate sectional planes. The user can also set the distance and the thickness for capturing projected objects and the width and height of the section. For this study a maximum projection of 30 meters was used in the ACD and B zone. Stepping through the sections, which all have the same orientation, a curve (polyline) was digitized outlining the general trend of the iron formation and massive sulfide bodies (Fig. 20). It became obvious while digitizing the orebody trends that a single lateral horizon for the iron formation cannot be interpreted from the drillcore data.

The volumes of interest (iso-surface) can be calculated by populating all the cells in the voxet with a value of the distance from the cell to the nearest iron formation or massive sulfide. An iso-surface can then be generated from these cells. The iso-surface meshes all the cells that represent the distance to the object and does not adhere to any geological constraints. Therefore it can overlap or enclose cells of other surface types, (e.g., an iso-surface for massive sulfides can encompass an iso-surface of iron formation). Although this method does not precisely define the orebody or the distribution of iron formation, it does provide a quick realistic visualization in the correct spatial orientation, providing useful general structural information. Fig. 21 shows the more tabular nature of the B zone compared to the ACD zone. This analysis represents the orebody and iron formation (to some extent) well enough to give a general trend, dip and plunge direction of the ore horizon.

The orientation of the massive sulfides and iron formation was also investigated by generating dip markers by using three local points representing contact between iron formation and another unit (Fig. 22). This is accomplished by displaying the drillcore lithological units in a thick section (approximately 100 m) and selecting three contact points to act as the control for a local solution of a plane. The three points are connected by a closed polygon, from which a surface can be generated (Fig. 22). Multiple surfaces of this type were generated for both the massive sulfides and iron formation contacts in the different zones. These dip surfaces compare favourably to the calculated iso-surfaces indicating that this method can be used with confidence where the data are more sparse (Fig. 23).

4.2 Relationships Interpreted from the Model

The general dip trend from the B and ACD zones were used to generate a thrust surface representing the thrust contact shown on Figure 3 (Fig. 24). This same dip can be used to project surface geology to depth. Projecting rock units to depth can aid in understanding what structural control can be influencing the iron formation and massive sulfide distributions.

Because the iron formation is not seen as a pervasive horizon it may be more useful to model another stratigraphic feature for which more reliable and better sampled data are available, such as the chloritic tuff layer. Using the imported cross sections recovered from the mine (Fig. 25), curves representing common geologic contacts can be connected from section to section. In this reconstruction the most useful boundary can be represented by the contact between the hanging-wall (quartz ± feldspar porphyry) and footwall (chloritic tuff) as mentioned in the beginning of this section.

The association of the chloritic tuff with the massive sulfide is well documented by many workers (McCutcheon, 1992; Peter, 2003; Peter and Goodfellow, 2003; Peter et al., 1993; Peter et al., 2003), and it can extend over 1.5 km away from the massive sulfides. In most cases it occurs in the footwall to the massive sulfides, but it is also seen above the massive sulfides in some areas possibly due to tectonic thrusting and complex folding.

Copper, lead and zinc assay values included in the drillcore data were also gridded so that high assay values and their spatial association could be easily visualized. The voxet used to determine distance to massive sulfides was used to calculate the distance to high Cu, Pb and Zn values. These properties can then be compared to the reconstructed orebodies. The assay values can also be displayed as point objects where they occur at depth (Fig. 26). The down-plunge continuity of the Cu, Zn, and Pb-rich sulfides in the B zone provide a clear indication of the possible 3-D structure of the hydrothermal up-flow zones (cf. Fig. 7), although this also could reflect local superimposed structure or remobilization. Both orebodies (Fig. 21), and the observed Cu-, Pb- and Zn-rich zones in the B zone (Fig. 26) plunge in a west-south west direction and closely follow the limbs and hinge zone of the North Little River Lake fold. The B zone is more tabular and ACD zone is thicker, which may be due to the proximity of the ACD zone to the hinge of the fold.

The data depicted in Figs. 21 and 26 are consistent with the strike and dip of the orebodies (de Roo et al., 1990a; McCutcheon, 1990; Moreton, 1994; Park, 1996; Wilson, 1993) noted in earlier studies, but greatly extend this information to depth (cf. Fig. 26) and provide additional data, such as metal zoning, to help identify possible deep extension of the up-flow zones. The tabular nature of the B zone makes the zoning easy to identify, but the difference in composition of B and ACD zone ore (cf. Table 1: ACD higher in Zn and Pb) is also clear. This information can help to target proximal copper-rich mineralization at depth.

From the airborne magnetic data, a good correlation is seen between the magnetic anomalies and drilled massive sulfide intersections (Fig. 27). It can also be seen that the massive sulfide body with the most abundant iron formation (B zone) has the largest magnetic anomaly amplitude. The other zones also have a magnetic signature that correlates with sulfide and iron formation intersections in the 3-D model. For the purpose of this study only a visual inspection was done with the magnetic data. Further studies such as anomaly signature versus volume and depth or spatial proximity of massive sulfide and iron formation are suggested along with integrating other geophysical data types.

Another useful regional scale exploration tool presented by Peter (2003), is a hydrothermal sedimentary index in the iron-rich lithologies. By combining lithogeochemical data, an equation was derived to vector towards massive sulfides,

$$HTSIX = \left(\frac{Fe}{Ti}\right) + \left(\frac{P}{Ti}\right) + \left(\frac{CO_2}{Ti}\right) + \left(\frac{Ba}{Ti}\right) + \left(\frac{Fe}{Mn}\right) + \left(\frac{Eu}{Eu^*}\right) + \left(\frac{1}{Ce/Ce^*}\right) + \frac{\sum(Ag, As, Au, kBi, CdCu, Hg, In, Pb, Sb, Sn, Tl, Zn)}{Ti}$$

(see Peter, 2003 for definition and explanation of equation).

His results for the Heath Steele area are plotted in 2-D at the drill-collar locations, shown in Gocad© in Fig. 28. This 2-D representation does not provide critical information about the subsurface extent of the anomalies that can be more readily seen in the 3-D model. These data were incorporated into the 3-D model of Heath Steele and displayed in their proper position down the drill hole where the sample was collected (Fig. 29). The symbol represents the data position and the size of the symbol is relative to the size of the index value. This hydrothermal sedimentary index can now also be displayed in the same model along with the Cu, Pb, and Zn assay values (Fig. 30), the iron formation and massive sulfide bodies or any other data available. The results show that the major geochemical anomalies analysed in drillcore from ore-related Fe-rich sediments are located at depths 5 to over 700 m below surface, and not at surface. The down-hole visualisation greatly enhances the accurate targeting of additional sampling and exploration drilling at depth.

5.0 Discussion and Recommendations

3-D modelling of exploration and mine data is a valuable tool in understanding a deposit and its environment. Interpretations based on such models can be more reliable than anything that can be achieved by a selection of representative drill holes because they are constrained by all of the available information in the mine environment rather than a subset of that data. Fig. 33 shows an interpreted cross section from Noranda in a 3-D context. The cross sections indicate very complex surfaces between the stratigraphic units that cannot be supported by the drillcore data. Thus, by combining field data and mine information into one environment, multiple experts can contribute their knowledge to improve the overall understanding of the deposit and importantly asses quality of earlier work.

An important deficiency of many mine models is that geological data is mainly gathered in a small area of interest, where the ore is. This results in clusters of data sets in parts of the model where exploration was likely focused and sparse data sets between these areas of interest. In the study presented here, the information used to create the model were an integration of both measured data and interpretations. Areas of high data resolution increase confidence in the interpretation of the massive sulfide body, but where data points were not as dense, interpretations are more speculative. Interpretation adds a degree of uncertainty in the model but can still populate areas of sparse data by extrapolating information. This uncertainty needs to be captured so that when speculative targets are considered weight is given to the measure of uncertainty. Greater positional accuracy can also be achieved with more sophisticated methods of transforming historical mine grid data to national accepted coordinates (i.e. by using rotation, translation and scaling instead of linear translation used in this study). The inclusion of mine plans and rock/ore extraction, even where the geology is interpreted, can also greatly enhance the model.

Although data may be retained from early phases of exploration and mine development, the context is often lost following closure of the mine and "keys" for integrating data, such as conversion grids and core-logging codes, may have to be re-established. The corporate memory for such details also has a short life span relative to the exploration history of a region (e.g., >50 years in many brownfields). This highlights the importance of recording and retaining such data in active exploration programs, which may precede mine development by many decades. It is recommended that government and industry come to some agreement of submitting or maintaining digital nationally georeferenced UTM core logs, using consistent procedures and core logging naming conventions.

The model presented in this study integrated historical surface and subsurface drillcore data, geological map interpretations, structural data measurements, and interpretative cross sections, with a modern digital elevation model, geophysical airborne magnetic data and lithogeochemical data. The model can now be expanded and improved by integrating new data and by applying new expert knowledge. An example was presented by projecting the recently developed hydrothermal sediment index data from surface to depth in the 3-D mine environment. New queries using old data also can be run in the model to identify gaps in the knowledge of the studied area (e.g., features that were never drilled), which can lead to new exploration targets.

There is a large learning curve when working in a 3-D environment. This study has identified one possible workflow that can be applied at any stage of exploration or mine development. The importance of creating and maintaining 3-D models of exploration and mining data has been well argued by other workers (Kirkham et al., 2006; McGaughey and Valle, 1997; Orlic, 1997). Exploration companies are achieving results; such as Falconbridge (now X-Strata) and their discovery of the deep Ansil West deposit and the Montbray showing in Noranda. They continue to use the 3-D environment on a daily basis for such tasks as data validation, target selection, deposit definition and preliminary ore calculation.

For future work on the Heath Steele model presented in this study, and other models that might be created for the Bathurst Mining Camp, the focus should be on deeper deposits. The deepest drill hole in the Heath Steele model extends to 1432 m. However, mining in other mature camps (e.g., Kidd Creek, La Ronde) now extends to nearly 3 km depth. Less than 50% of the ore in Kidd Creek was mined from above 1 km. 3-D models of the type presented here are the essential framework in the deep search for new resources in these environments.

Future studies can also integrate airborne, ground and borehole geophysical data collected at and around Heath Steele utilizing the 3-D dataset presented from this study to evaluate their potential use in mineral exploration. The geophysical data can also be used to find tune contacts, structure and rock properties of the geological units.

6.0 Conclusions

By integrating drill core, regional maps, structural fabric measurements, rock geochemistry and geophysical data in a 3-D environment a new approach to visualizing the data has been presented along with several massive sulfide models of the Heath Steele deposit. The initial purpose of this study was to use the 3-D dataset to test the stratigraphic and spatial relationship of the iron formation to the massive sulfide bodies. However, it was apparent that using the drillcore data that iron formation was not going to more accurately vector to the massive sulfide bodies within the study area. In the B zone massive sulfide deposits, there is a significant unit of iron formation structurally overlaying the massive sulfide but in the ACD zone the iron formation is not closely spatially related to ore, and in fact there are many occurrences of iron formation in the drillcore data that are not spatially related to massive sulfides. This is seen in a distance map of the massive sulfides to the iron formation for both zones in Fig. 31.

The structural complexity at the mine scale of Heath Steele and inadequate distinction between iron formation and other lithologies in the historical core log makes it difficult to prove conclusively that there is a direct spatial association of iron formation with the massive sulfide. Therefore, other stratigraphic markers better represented in the drillcore data should be investigated as possible vectors to support exploration. Whereas data for the iron formation in the present model lacks continuity, the contact between the hanging-wall (quartz ± feldspar porphyry) and footwall (chloritic tuff) provides a more reliable 3-D representation of the modelled surfaces containing the ore horizon (Fig. 32).

Metal zonation of the modelled ore zones also provides a useful indication of the locus of hydrothermal up-flow and possible ore-controlling structures. The strong linear zones of Cu-rich ore in the B zone suggest proximity to high-temperature up-flow, whereas the Pb and Zn-rich nature of the ACD zones suggest a more distal setting. Although the representation of the iron formation in the model is not continuous enough to establish a clear spatial relationship to ore across the Heath Steele mines, geochemical anomalies within the documented volumes of iron formation provide useful indicators of proximity to up-flow zones (Peter, 2003) in a regional context.

Structural control on the units and the orebodies is key to understanding where additional deposits or extensions of mine deposits might be located. This could be achieved by a more rigorous analysis of dip markers of the type presented in this study (Fig. 22 and 23). By extending F_1 and/or F_2 folds and plunge direction of the massive sulfide body, predictions can be made how the current ore body continues down depth.

Other applications of the model not tested in this study include possible alteration vectors that may highlight prospective and, as yet, untested volumes in the model. Further geochemical studies presented in a 3-D context can also help clarify the association of the massive sulfides and the chloritic tuff (e.g., alteration vectors). Caution must be used when using data relationships such as geochemistry, that the data has been treated carefully and with knowledge of its derivation (Grunsky, 2007). Using 'bad' data, one could over or under represent a key relationship, but by investigating the data in a 3-D context these relationships may be easier to interpret.

The success of surficial magnetics and EM surveys also suggest that down-hole geophysical surveys would be valuable and useful if modelled in the new 3-D framework to target deeper drilling such as research done at other deposits in the Bathurst Mining Camp (Mwenifumbo et al., 2003).

References:

Authur, M., and Sageman, B. B., 1994, Marine Shales: Depositional mechanisms and environments of ancient deposits: Annual Review of Earth and Planetary Science, v. 22, p. 499-551.

Bevier, M. L., 1988, U-Pb geochronologic studies of igneous rocks in New Brunswick, *in* Abbott, S. A., ed., Thirteenth annul review of activities, project resumes. New Brunswick, Department of Natural Resources and Energy, p. 134 - 140.

Bonham-Carter, G.F., 1994, Geographic information systems for geoscientists: modelling with GIS, *in* Merriam, D. F. ed., Computer methods in the geosciences, 13, p. 337.

de Kemp, E. A., and Sprague, K. B., 2003, Interpretive tools for 3-D structural geological modeling part I: bezier-based curves, ribbons and grip frames: GeoInformatica, v. 7, p. 55-71.

de Roo, J. A., Moreton, C., and Williams, P. F., 1990a, Structure of the Heath Steele deposits, *in* Fyffe, L. R., ed., Field Guide to Massive Sulphide Deposits in Northern New Brunswick: Fredericton, Minerals and Energy Division, Department of Natural Resource and Energy, New Brunswick, p. 84-101.

de Roo, J. A., Moreton, C., Williams, P. F., and van Staal, C. R., 1990b, The structure of the Heath Steele Mines region, Bathurst Camp, New Brunswick: Atlantic Geology, v. 26, p. 27-41.

de Roo, J. A., and van Staal, C. R., 1994, Transpression and recumbent folding: steep belts and flat belts in the Appalachian Mobile Belt of northern New Brunswick, Canada: Geological Society of America Bulletin, v. 106, p. 541-552.

de Roo, J. A., and van Staal, C. R., 2003, Sulfide remobilization and sulfide breccias in the Heath Steele and Brunswick deposits, Bathurst Mining Camp, New Brunswick, *in* Goodfellow, W. D., McCutcheon, S. R., and Peter, J. M., eds., Massive Sulfide Deposits of the Bathurst Mining Camp, New Brunswick and Northern Maine, Economic Geology Monograph 11, p. 479-496.

de Roo, J. A., Williams, P. F., and Moreton, C., 1991, Structure and evolution of the Heath Steele base metal sulfide orebodies, Bathurst camp, New Brunswick, Canada: Economic Geology, v. 86, p. 927-943.

Dechow, E. W. C., 1959, The geology of the Heath Steele Mine, Newcastle, New Brunswick: Unpub. PhD thesis, Yale University, 191 p.

ed. Goodfellow, W. D., McCutcheon, S. R., and Peter, J. M., 2003, Massive Sulfide Deposits of the Bathurst Mining Camp, New Brunswick, and Northern Maine, XX p.

Goodfellow, W. D., 2002, Current Understanding of the origin of massive sulphide deposits in the Bathurst Mining Camp, Northern New Brunswick., The Gangue.

Goodfellow, W. D., and McCutcheon, S. R., 2003, Geological and genetic attributes of volcanic-associated massive sulfide deposits of the Bathurst Mining Camp, northern New Brunswick - a synthesis, *in* Goodfellow, W. D., McCutcheon, S. R., and Peter, J. M., eds., Massive Sulfide Deposits of the Bathurst Mining Camp, New Brunswick, and Northern Maine, Economic Geology Monograph 11, p. 245-301.

Goodfellow, W. D., McCutcheon, S. R., and Peter, J. M., 2003a, Massive sulfide deposits of the Bathurst Mining Camp and northern Maine; introduction and summary of findings, *in* Goodfellow, W. D., McCutcheon, S. R., and Peter, J. M., eds., Massive

Sulfide Deposits of the Bathurst Mining Camp, New Brunswick and Northern Maine, Economic Geology Monograph 11, p. 1-16.
Goodfellow, W. D., McCutcheon, S. R., and Slack, J. F., 2003b, Massive sulfide deposits of the Bathurst Mining Camp and northern Maine; introduction and summary of findings, *in* Goodfellow, W. D., McCutcheon, S. R., and Peter, J. M., eds., Massive Sulfide Deposits of the Bathurst Mining Camp, New Brunswick and Northern Maine, Economic Geology Monograph 11, Economic Geology Publishing Company.
Goodfellow, W. D., Peter, J. M., Winchester, J. A., and van Staal, C. R., 2003c, Ambient marine environment during formation of massive sulfide deposits of the Bathurst Mining Camp: importance of reduced bottom waters in metal precipitation and sulfide preservation, *in* Goodfellow, W. D., McCutcheon, S. R., and Peter, J. M., eds., Massive Sulfide Deposits of the Bathurst Mining Camp, New Brunswick, and Northern Maine, Economic Geology Monograph 11, p. 129-156.
Grunsky, E. C., 2007, The Evaluation of Geochemical Survey Data: Data Analysis and Statistical Methods Using Geographic Information Systems, *in* Harris, J., ed., GIS for the Earth Sciences, Special Publication 44, GSC, p. 229-283.
Kirkham, G. D., Falck, H., and Siddorn, J. P., 2006, An integrated 3-D GIS model of the Yellowknife camp: a tool for efficient development, *in* Anglin, C. D., Falck, D. F., Wright, D. F., and Ambrose, E. J., eds., Gold in the Yellowknife greenstone belt, Northwest Territories: Results of the EXTECH III Multidisciplinary Research Project, Special Publication No. 3, Geological Association of Canada, Mineral Deposits Division, p. 362-371.
Luff, W. M., 1995, A history of mining in the Bathurst area, northern New Brunswick, Canada: Canadian Institute of Mining and Metallurgy Bulletin, v. 88, p. 63 - 68.
McBride, D. E., 1976, The structure and stratigraphy of the B-zone, Heath Steele Mines, Newcastle, New Brunswick: Unpub. Ph.D. thesis, University of New Brunswick, 227 p.
McCutcheon, S. R., 1990, Base metal deposits of the Bathurst-Newcastle District, *in* Fyffe, L. R., ed., Field Guide to Massive Sulphide Deposits in Northern New Brunswick: Fredericton, New Brunswick, Department of Natural Resources and Energy, p. 42-71.
McCutcheon, S. R., 1992, Base-metal deposits of the Bathurst-Newcastle district: characteristics and depositional models: Exploration and Mining Geology, v. 1, p. 105-119.
McCutcheon, S. R., Fyffe, L. R., Gower, S. J., Langton, J. P., Wilson, R. A., Lentz, D., Langton, J. P., Walker, J. A., Hamilton, A., and Luff, W. M., 1997, Geology and Massive Sulphide Deposits of the Bathurst Camp, New Brunswick, *in* McCutcheon, S. R., ed., Geological Association of Canada, Mineralogical Association of Canada, Field Trip B7 Guidebook: Ottawa, Geological Association of Canada, p. 1-27.
McCutcheon, S. R., Langton, J. P., van Staal, C. R., and Lentz, D. R., 1993, Stratigraphy, tectonic setting and massive-sulphide deposits of the Bathurst Mining Camp: Bathurst '93, Third Annual Field Conference, Bathurst, New Brunswick, 1993, Application of Recent Geological Concepts to Exploration in the Northern Appalachians, p. 1-39.
McCutcheon, S. R., Luff, W. M., and Boyle, R. W., 2003, The Bathurst Mining Camp, New Brunswick, Canada: history of discovery and evolution of geological models,

in Goodfellow, W. D., McCutcheon, S. R., and Peter, J. M., eds., Massive Sulfide Deposits of the Bathurst Mining Camp, New Brunswick, and Northern Maine, Economic Geology Monograph 11, p. 17-35.

McGaughey, W. J., and Valle, M. A., 1997, Ore delineation in three dimensions, *in* Gubins, A. G., ed., Proceedings of Exploration97: Decennial International Conference on Mineral Exploration, p. 639-650.

Moreton, C., 1994, The stratigraphy, structure and geometry of the B, B5 and E zone massive sulphide deposits, Heath Steele Mines, Newcastle, New Brunswick: Unpub. Ph.D. thesis, University of New Brunswick, Fredricton, 398 p.

Mwenifumbo, C. J., Elliott, B. E., and Street, P., 2003, Borehole geophysical characteristics of massive sulphide deposits in the Bathurst Mining Camp, *in* Goodfellow, W. D., McCutcheon, S. R., and Peter, J. M., eds., Massive Sulfide Deposits of the Bathurst Mining Camp, New Brunswick, and Northern Maine, Economic Geology Monograph 11, p. 841-860.

Orlic, B., 1997, Predicting Subsurface Conditions for Geotechnical Modelling: Unpub. Ph. D. thesis, University of Technology, Delft, Netherlands, 165 p.

Park, A. F., 1996, Geology and structural analysis of the A, C, N-3, N-6 and N-5 zones at Heath Steele mines and the Stratmat Boundary zone (part of NTS 21 0/8 east), Northern New Brunswick, Open File Report 96-17, Natural Resources and Energy New Brunswick.

Peter, J. M., 2003, Ancient iron formations: their genesis and use in the exploration for stratiform base metal sulphide deposits, with examples from the Bathurst Mining Camp, *in* Lentz, D. R., ed., Geochemistry of Sediments and Sedimentary Rocks: Evolutionary Considerations to Mineral Deposit-forming Environments, Geological Association of Canada, Geotext 4, p. 145-176.

Peter, J. M., and Goodfellow, W. D., 1996, Mineralogy, bulk and rare earth element geochemistry of massive sulphide-associated hydrothermal sediments of the Brunswick horizon, Bathurst mining camp, New Brunswick: Canadian Journal of Earth Sciences, v. 33, p. 252-283.

Peter, J. M., and Goodfellow, W. D., 2003, Hydrothermal sedimentary rocks of the Heath Steele Belt, Bathurst Mining Camp, New Brunswick 3. Application of mineralogy and mineral and bulk composition to massive sulfide exploration, *in* Goodfellow, W. D., McCutcheon, S. R., and Peter, J. M., eds., Massive Sulfide Deposits of the Bathurst Mining Camp, New Brunswick, and Northern Maine, Economic Geology Monograph 11, p. 417-433.

Peter, J. M., Goodfellow, W. D., Davies, J. F., Gibson, H. L., and Whitehead, R. E. S., 1993, Geochemistry of massive-sulfide-associated hydrothermal sediments of the Brunswick Belt, Bathurst, New Brunswick *in* Third annual field conference of the Geological Society of CIM; papers: Exploration and Mining Geology, v. 2, p. 428.

Peter, J. M., Kjarsgaard, I. M., and Goodfellow, W. D., 2003, Hydrothermal sedimentary rocks of the Heath Steele Belt, Bathurst Mining Camp, New Brunswick: Part1. Mineralogy and mineral chemistry, *in* Goodfellow, W. D., McCutcheon, S. R., and Peter, J. M., eds., Massive Sulfide Deposits of the Bathurst Mining Camp, New Brunswick, and Northern Maine, Economic Geology Monograph 11, p. 361-390.

Rogers, N., and van Staal, C. R., 2003, Volcanology and tectonic setting of the northern Bathurst Mining Camp: Part II - mafic volcanic constraints on back-arc opening, *in* Goodfellow, W. D., McCutcheon, S. R., and Peter, J. M., eds., Massive Sulfide

Deposits of the Bathurst Mining Camp, New Brunswick, and Northern Maine, Economic Geology Monograph 11, p. 181-201.
Skinner, R., 1974, Geology of Tetagouche Lakes, Bathurst and Nepisiguit Falls map areas, New Brunswick: Geol. Surv. Can. Mem., v. 371, p. 133.
Spry, P. G., Peter, J. M., and Slack, J. F., 2000, Meta-exhalites as exploration guides to ore, Metamotphic and Metamorphogenic Ore Deposits, 11, Reviews in Economic Geology, p. 163-201.
van Staal, C. R., 1987, Tectonic setting of the Tetagouche Group in northern New Brunswick: implications for plate tectonic models of the northern Appalachians: Canadian Journal of Earth Sciences, v. 24, p. 1329-1351.
van Staal, C. R., 1994a, Brunswick subduction complex in the Canadian Appalachians: record of Late Ordovician to Late Silurian collision between Laurentia and the Gander margin of Avalon: Tectonics, v. 13, p. 946-962.
van Staal, C. R., 1994b, Geology, Brunswick Mines, New Brunswick: Geological Survey of Canada, Map 1836a.
van Staal, C. R., Fyffe, L. R., Langton, J. P., and McCutcheon, S. R., 1992, The Ordovician Tetagouche Group, Bathurst camp, northern New Brunswick, Canada: History, tectonic setting, and distribution of massive-sulfide deposits: Exploration and Mining Geology, v. 1, p. 93-103.
van Staal, C. R., and Luff, W. M., 1990, The Brunswick No. 12 and No. 6 mines, Brunswick Mining and Smelting Corporation Limited, *in* Fyffe, L. R., ed., Field Guide to Massive Sulphide Deposits in Northern New Brunswick: Fredericton, Minerals and Energy Division, Department of Natural Resource and Energy, New Brunswick, p. 72-83.
van Staal, C. R., and Williams, P. F., 1984, Structure, origin and concentration of the Brunswick 12 and 6 orebodies: Economic Geology, v. 79, p. 1669-1692.
van Staal, C. R., Wilson, R. A., Fyffe, L. R., Langton, J. P., McCutcheon, S. R., Rogers, N., McNicoll, V., and Ravenhurst, C. E., 2003a, Geology and tectonic setting of the Bathurst Mining Camp and its relationship to coeval rocks in southwestern New Brunswick and adjacent Maine - a synthesis, *in* Goodfellow, W. D., McCutcheon, S. R., and Peter, J. M., eds., Massive Sulfide Deposits of the Bathurst Mining Camp, New Brunswick, and Northern Maine, Economic Geology Monograph 11, p. 37-60.
van Staal, C. R., Wilson, R. A., Rogers, N., Fyffe, L. R., Gower, S. J., Langton, J. P., McCutcheon, S. R., and Walker, J. A., 2003b, A New Geological Map of the Bathurst Mining Camp and Surrounding Areas - A Product of Integrated Geological, Geochemical and Geophysical Data, *in* Goodfellow, W. D., McCutcheon, S. R., and Peter, J. M., eds., Massive Sulfide Deposits of the Bathurst Mining Camp, New Brunswick, and Northern Maine, Economic Geology Monograph 11, p. 61-64.
Vander Most, A., and de Kemp, E. A., 2006, Increasing Interpretive Potential and Mineral Prospectivity through 3D Interpretive Mapping, Wealth Creation in the Minerals Industry: Integrating Science, Business and Education: Keystone, Co, Society of Economic Geologist, Inc. .
Vander Most, A., de Kemp, E. A., Hannington Mark, D., Goodfelloow, W. D., and Peter, J. M., 2007, New eyes on old data: A 3-D historical data integration study in the Heath Steele mining camp, Bathurst New Brunswick, Canada, Exploration 07: Toronto, ON, CA.

Williams, H., 1979, Appalachian Orogen in Canada: Canadian Journal of Earth Science, v. 16, p. 792-807.

Wilson, R. A., 1992, Bedrock geology of the Heath Steele-Halfmile Lake area, Bathurst Camp, northern New Brunswick, Devono-Carboniferous magmatism, deformation, metamorphism and related mineralization in the Atlantic Provinces: Current Research in the Atlantic Provinces, v.28. Atlantic Geology: Fredericton, NB, Canada, Atlantic Geoscience Society, p. 211.

Wilson, R. A., 1993, Geology of Heath Steele-Halfmile Lakes Area; Northumberland County, New Brunswick, *in* Resources, N. R. a. E. M., ed., Report of Investigation 25, Department of Natural Resources and Energy Province of New Brunswick, p. 98.

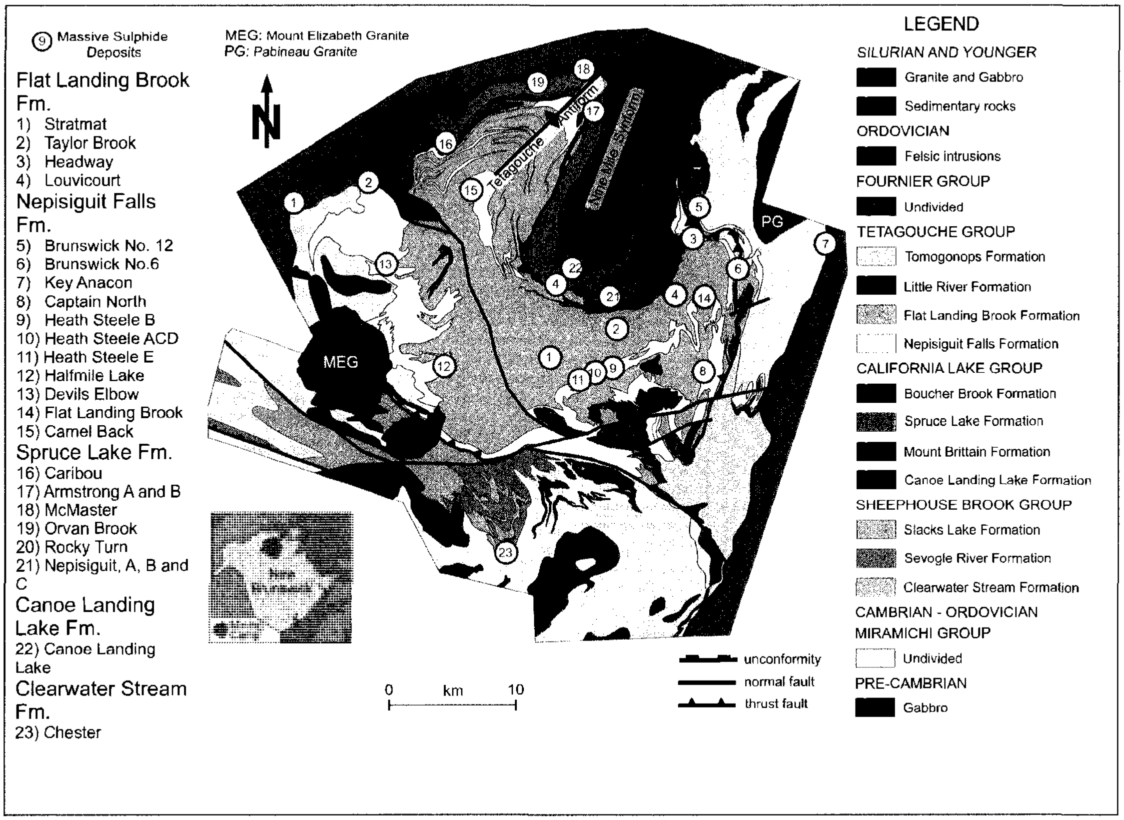

Figure 1. Massive sulfide deposits shown within prospective formations of the different geological groups of Bathurst Mining Camp, New Brunswick (from van Staal et al., 2003)

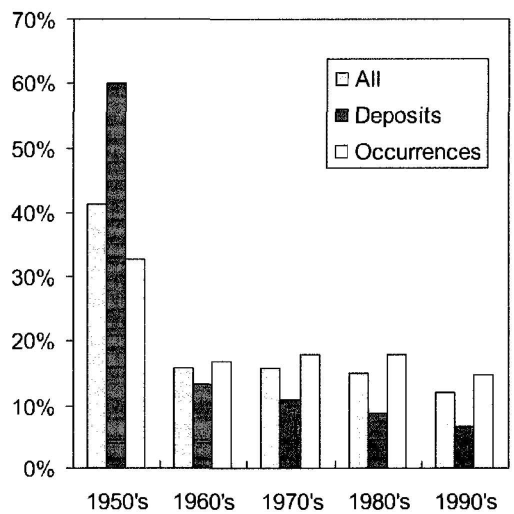

Figure 2. Volcanogenic massive sulphide (VMS) occurrences, deposits and combined deposit and occurrence discoveries shown as percentages for the Bathurst Mining Camp for a fifty year period after the first major massive sulfide discovery in 1952 (from McCutcheon et al., 2003).

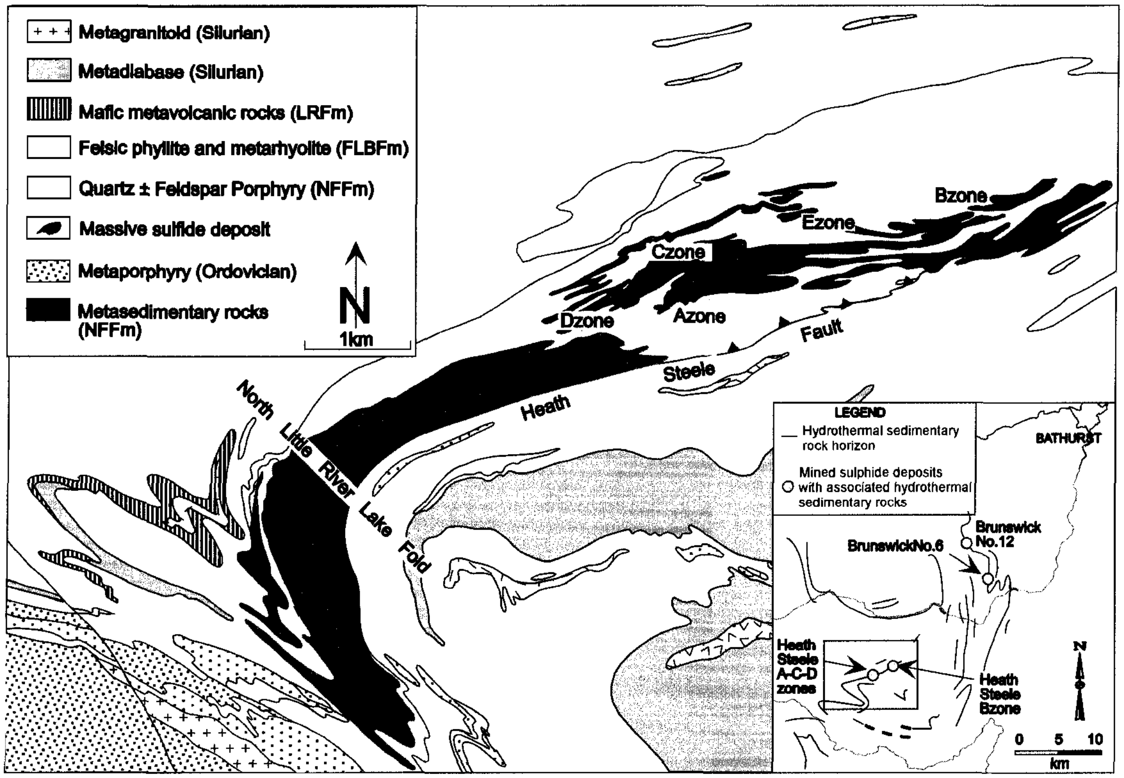

Figure 3. Locations of the A, B, C, D and E ore zones on the Heath Steele property. ACD zones are closer to the North Little River Lake fold hinge where the B and E zones are further out on the north limb of the fold (from Peter and Goodfellow, 2003).

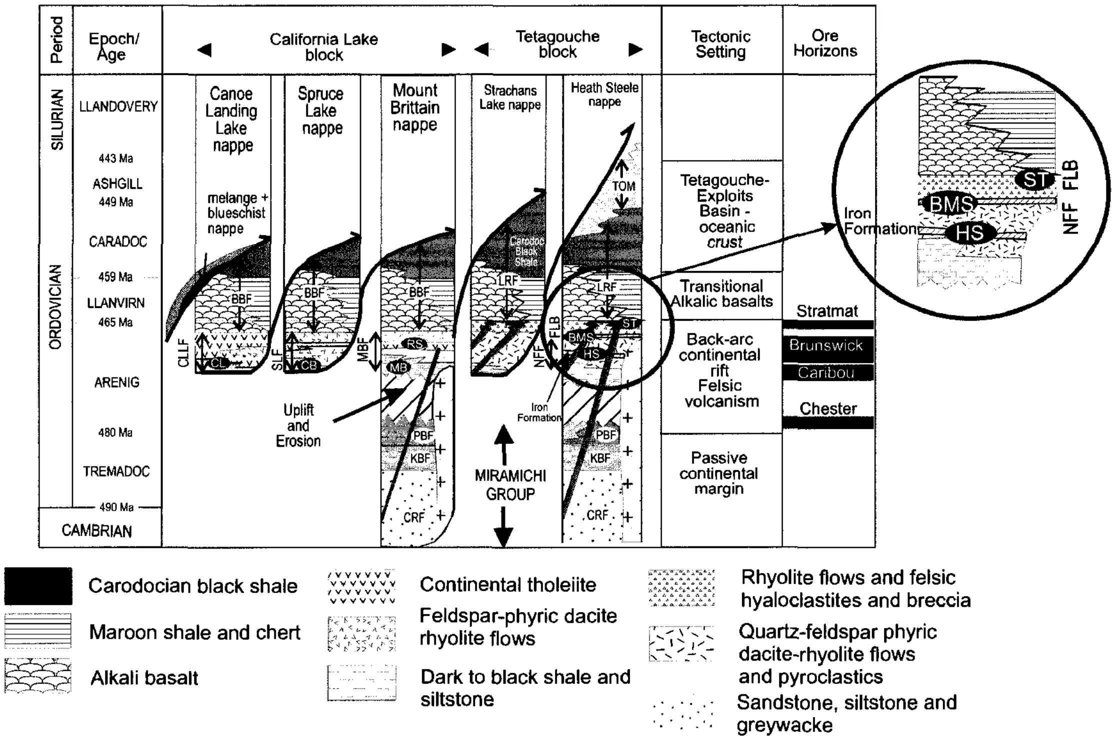

Figure 4. General stratigraphic columns indicating the thrust blocks and position of the ore horizons hosted by the Canoe Landing Lake (CLLF), Flat Landing Brook (FLB), Nepisiguit Falls (NFF), Mount Brittain (MBF) and Spruce Lake (SPF) Formations. Heath Steele occurs in the Nepisiguit Falls Formation at the contact between the sedimentary rocks and quartz-feldspar porphryrtic rocks (from van Staal et al, 2003). Red points represent the spatial context of some of the economical deposits of the Bathurst Mining Camp: Canoe Landing lake (CL), Caribou (CB), Murray Brook (MB), Restigouche (RS), Brunswick 6 and 12 (BMS), Heath Steele (HS), and Stratmat (ST). Other abbreviations: Boucher Brook (BBF), Clear Stream (CRF), Knights Brook (KBF), Patrick Brook (PBF), Little River (LRF), and Tomogonops (TOM) Formations.

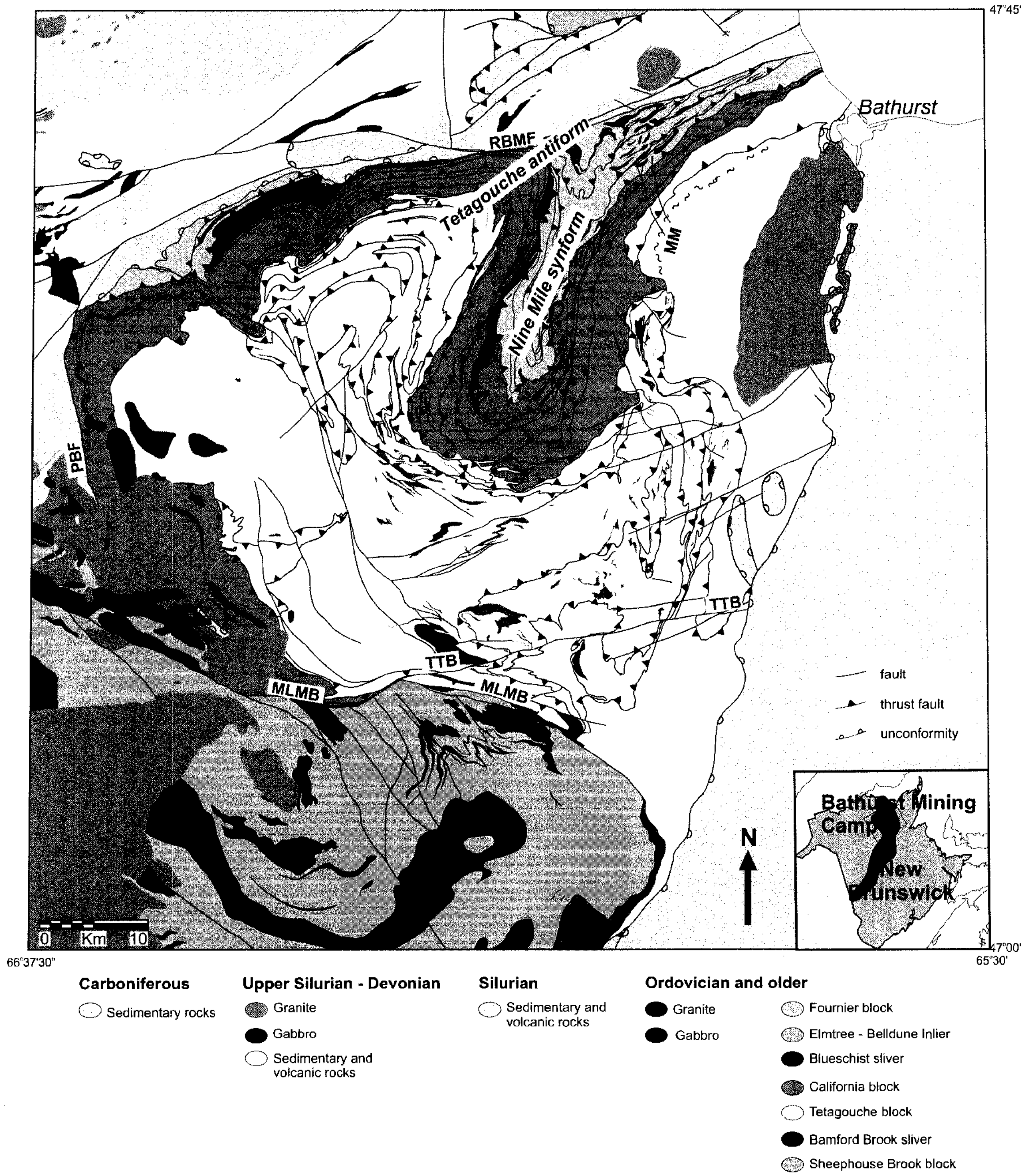

Figure 5. Map displaying the distribution of the major structures and tectonic blocks in the Bathurst Mining Camp (modified from van Staal et al., 2003). Abbreviations: Miramichi melange (MM), Moose Lake-Mountain Brook fault (MLMB), Portage Brook fault (PBF), Rocky Brook Millstream fault system (RBMF), and Tomogonops-Tozer Brook fault (TTB).

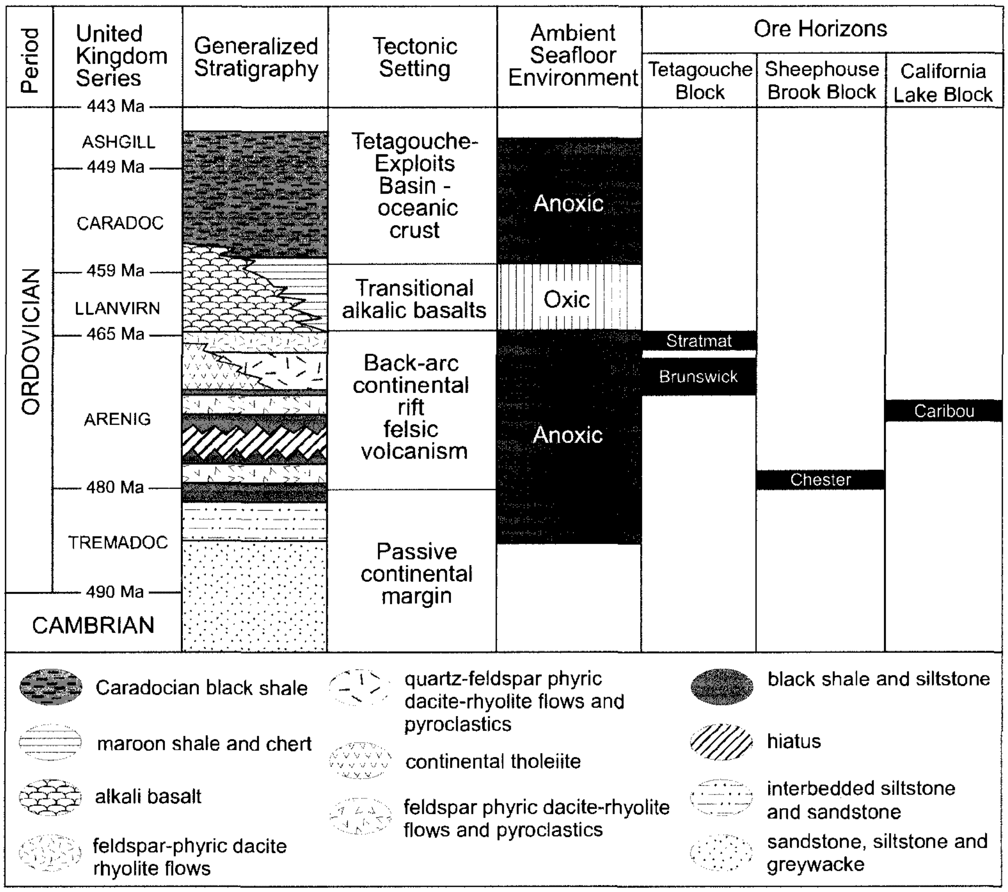

Figure 6. Redox conditions during ore horizon deposition in the Tetagouche, Sheephouse Brook and California Lake Blocks of the Bathurst Mining Camp. A general stratigraphic column is also shown along with the tectonic setting (from Goodfellow and McCutcheon, 2003). The Heath Steele deposit occurs near the bottom of the Brunswick Ore horizon.

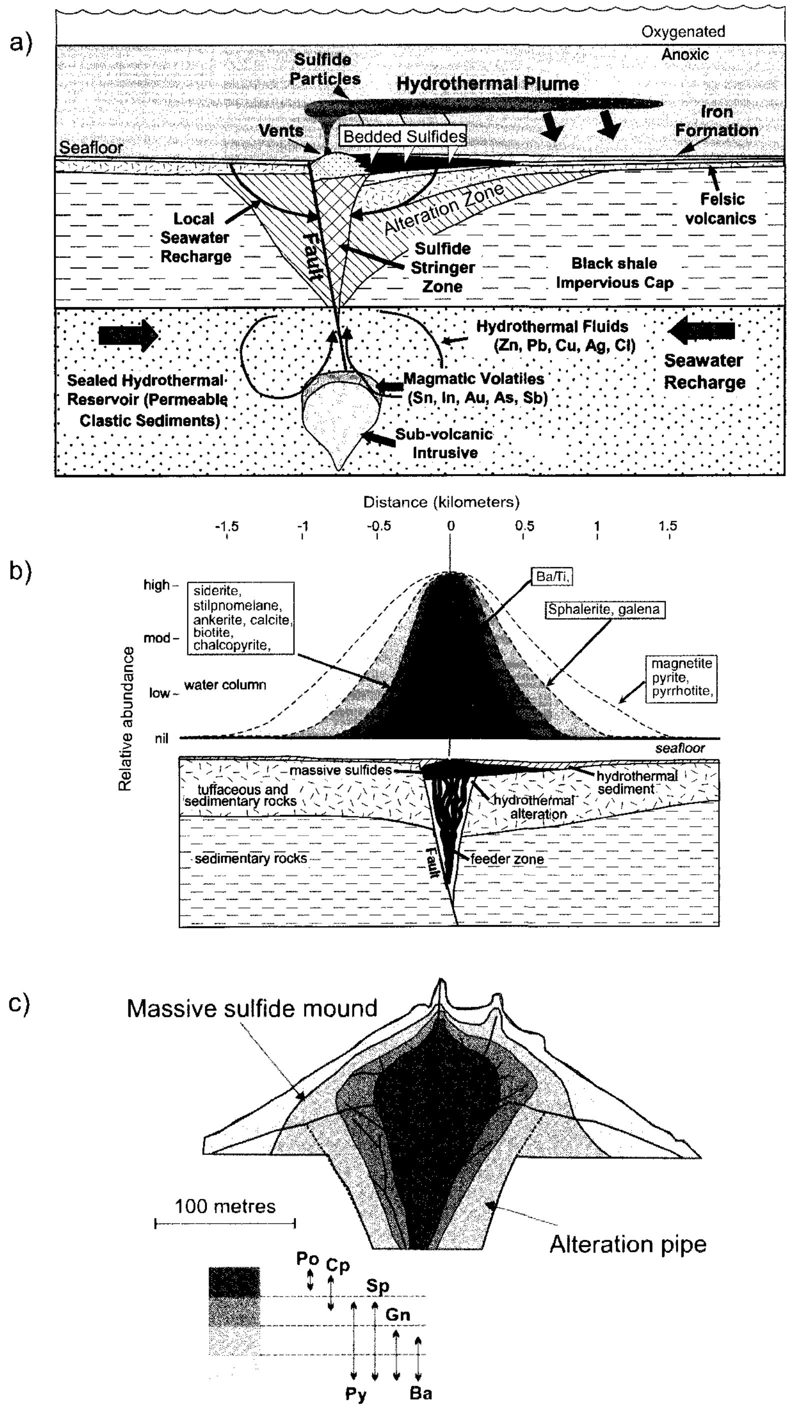

Figure 7. (a). Detailed view of hydrothermal system showing fluid driven by magma convection, leaching of host rocks, alteration surrounding the sulfide stringer zone, venting of hydrothermal fluids and zoning of sulfides. (b). Relative abundance and lateral extent of sulfide zoning around hydrothermal vents (from Goodfellow and McCutcheon, 2003). (c). Temperature and composition of hydrothermal fluids are a function to mineral zonation within VMS, where core of the vent precipitate Pyrrotite (Po) and Chalcopyrite (Cp) where it is hotter and Galena (Gn) and Sphalerite (Sp) further out where temperatures are cooler (from Galley et al., 2007).

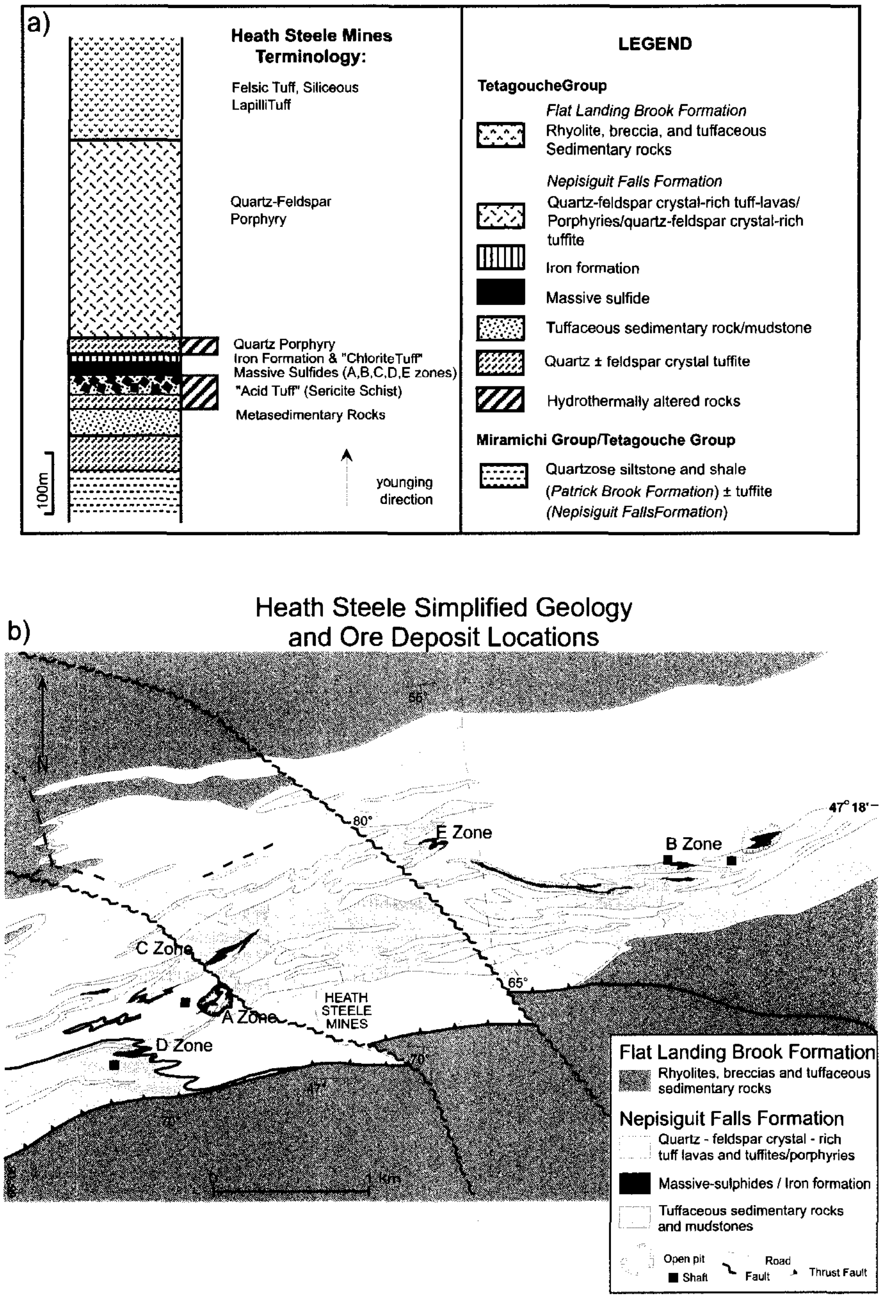

Figure 8. (a). Detailed column of the Heath Steele area (modified by Peter et al., 2003). (b). Simplified geology map of the Heath Steele property and locations of the ACD, B and E zones. The Nepisiguit Falls Formation hosts the ore deposits and is stratigraphically bound by the Flat Landing Brook Formation.

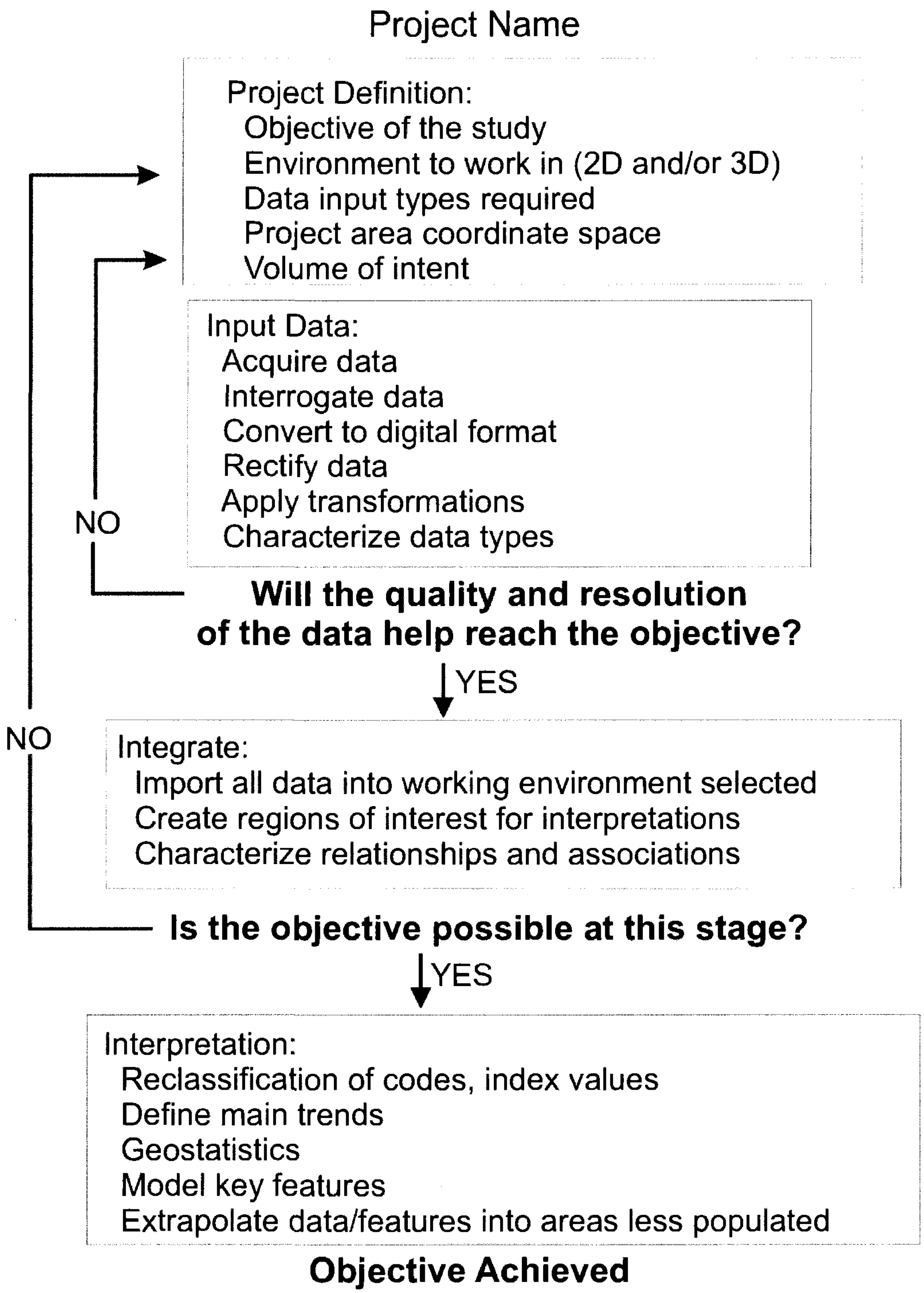

Figure 9. Summary of workflow developed in this study for creating an exploration model in a 2-D and/or 3-D environment. The objective of the project should be re-examined many times while developing the model to ensure that it is the correct objective and it can be achieved.

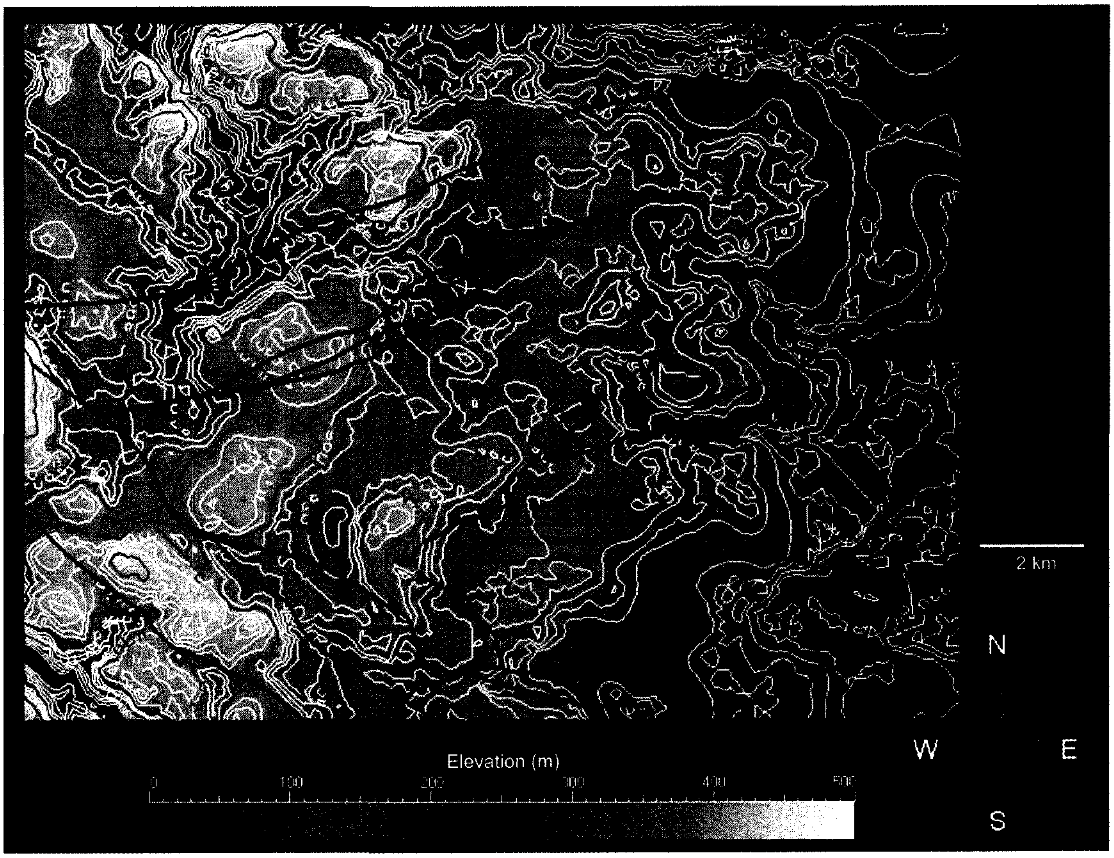

Figure 10. The digital evaluation model (DEM) complied for Heath Steele property gridded in ArcMap© from point data provided by Noranda. The general elevation is 375 meters above sea level with the largest gradient increases to the west towards the Miramichi Highlands. The thick black lines are normal faults and thrust faults from van Staal et al. (2003) and the red outlines are the Heath Steele deposit zones from de Roo et al. (1990). Distance across from West to East is approximately 18 km.

Figure 11. Autocad drawing file, shown in blue, is overlaid on and "rubber-sheeted" to the orthometric photo by using common roads and man-made structures. The origin point of the Autocad drawing file was then able to be read directly from the orthometric photo.

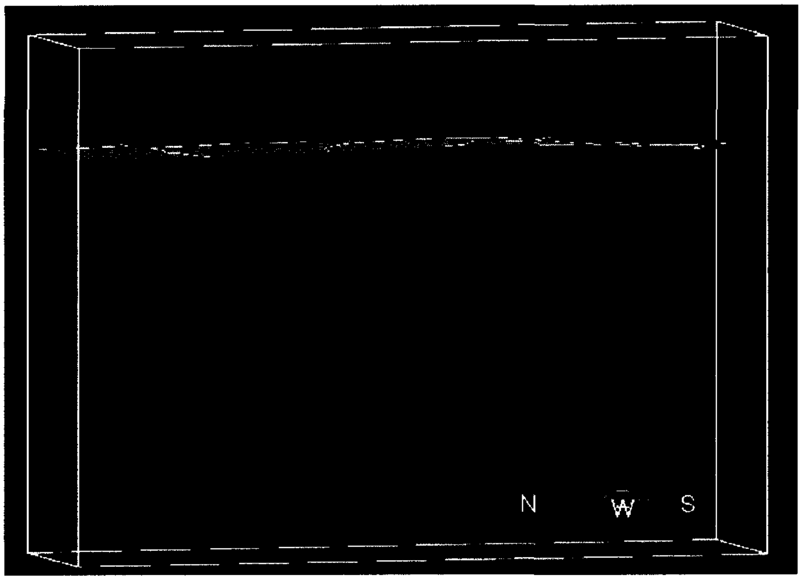

Figure 12. Example of subsurface drill pathways displayed in a 3-D environment. View is looking West, North is to the left. Section of DEM is displayed to indicate the surface. Size of view is a clipped set of data where the cube containing the data is 2.2 km long, 1.6 km deep and .64 km wide. The deepest drill core displayed is 1 km straight down from surface or approximately 1.15 km along the drill pathway.

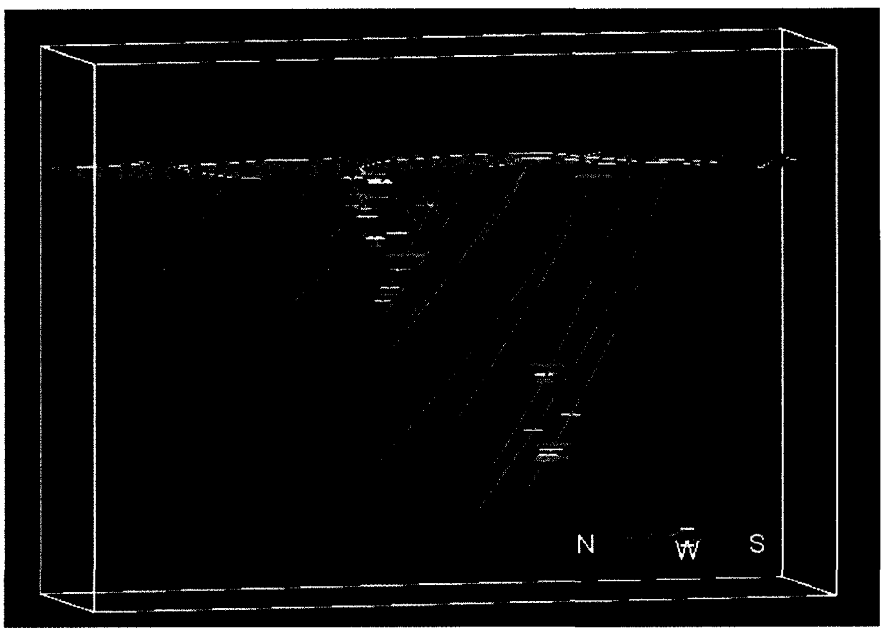

Figure 13. Same image as Fig. 12 with drill path and indicating the rock code. Each colour represents a different lithology as cited in the core logging database. The yellow disks show bottom markers for massive sulfides and the purple are bottom markers for iron formation as cited by the core logging database and read by the Gocad© input wizard. By converting the properties to curves they can be treated as objects that can then be queried to create regions of specific targeted data.

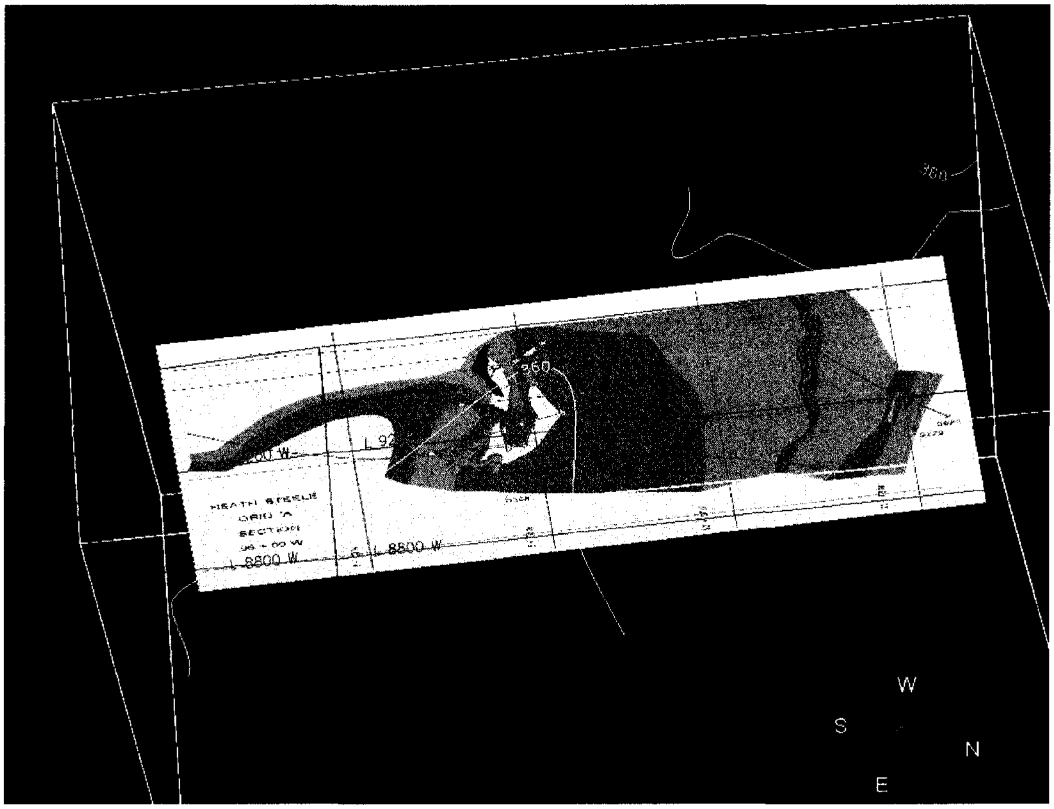

Figure 14. Example of an imported 2-D interpreted cross section (96 + 00 N) from the ACD zone constructed by Noranda geologists. The cross section represents a view 845 m across and 270 m deep. A transparent view of the DEM is displayed with white contour lines and was used to inspect the accuracy of the location of the cross section in its z component. The Heath Steele mine grid is also displayed in red. The cross sections sits right on the 96 + 00 grid line (the mine grid in this image has been transformed to UTM NAD83 zone 19N).

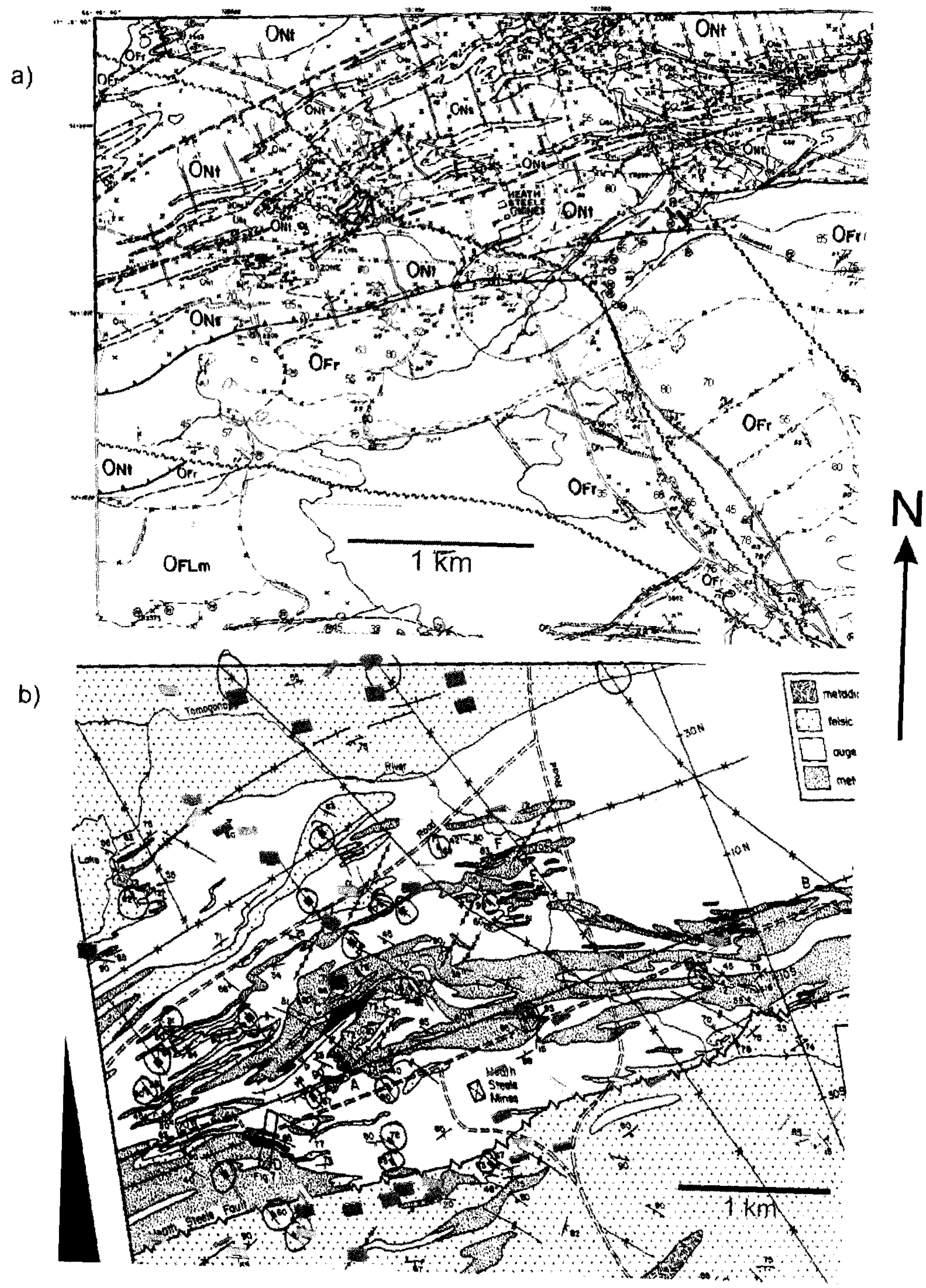

Figure 15. (a) Example of a portion of a hard copy geology map scanned and rectified in ArcMap© (2-D environment). The red structural markers are the result of digitizing the structural markers from the map using an ArcMap© tool called "Dig-Sym". (b) These shape files from ArcMap© were then converted to Gocad© 3-D objects. Gocad© can read trend and dip properties from objects and assign them as structural features. Shown in (b) is the D1 structural marker from de Roo et al (1990) where the yellow side is the top and green is the underside. The tablets are aligned with the strike direction and dip according to the dip property assigned to the point.

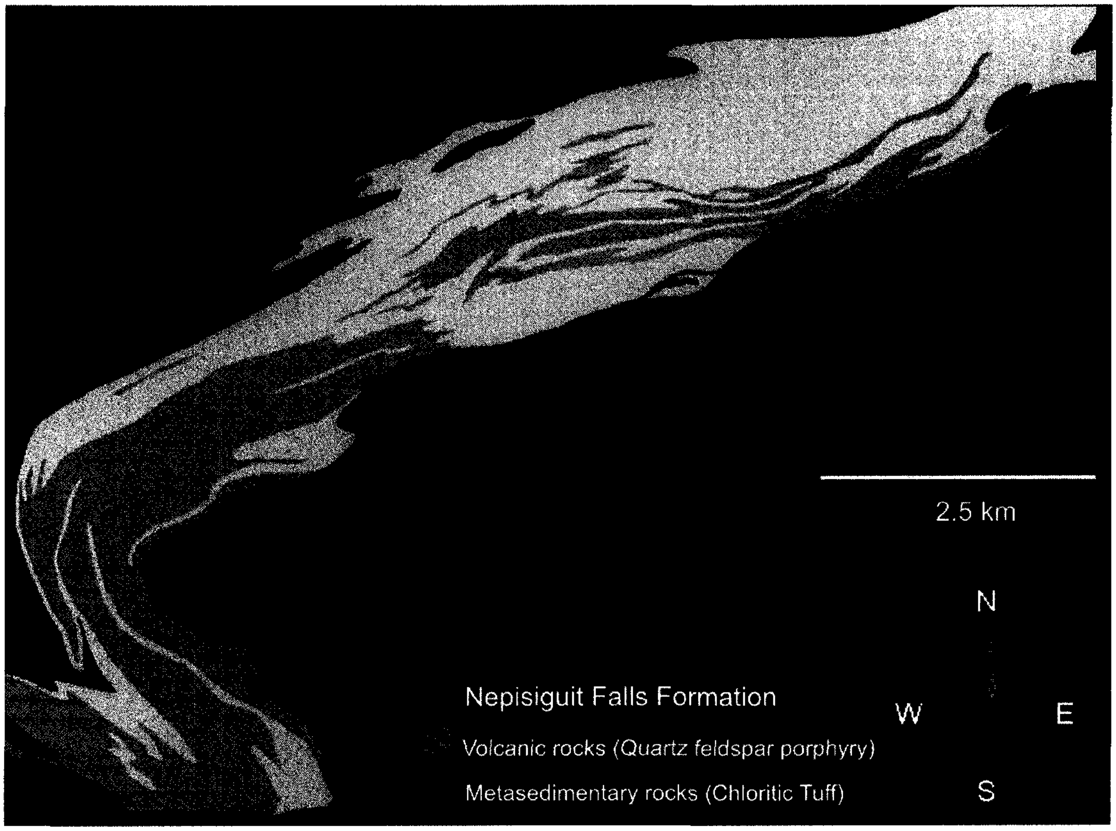

Figure 16. Example of a geology Gocad© surface. The regional geology map was brought into Gocad© then divided up into different surface objects according to their unique geology. This allows the user to display the individual geology surfaces as they are needed. Shown is the volcanic rocks (quartz feldspar porphyry) and metasedimentary rocks (chloritic tuff) of the Nepisiguit Falls Formation (rock names are mine terminology).

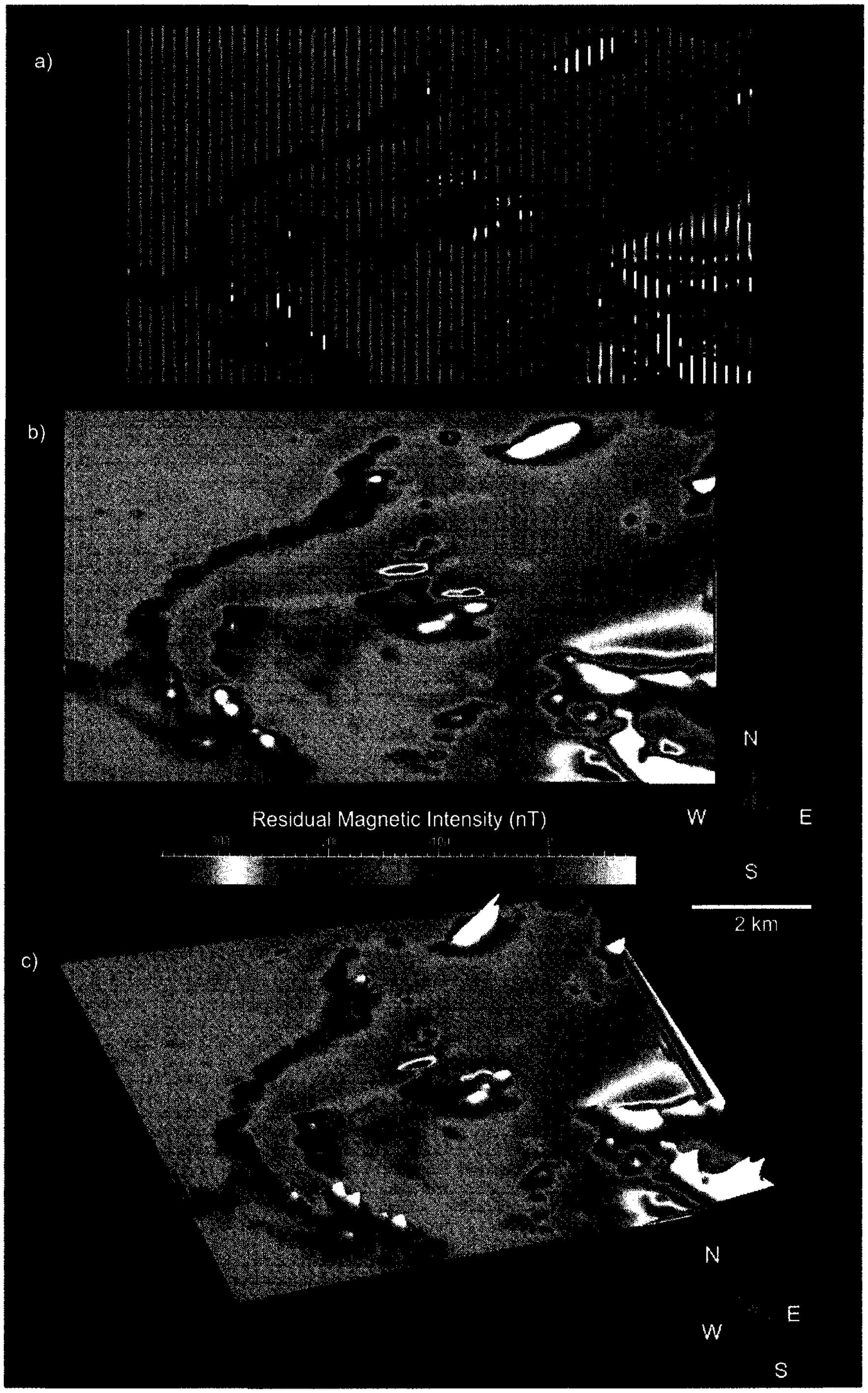

Figure 17. a) Airborne residual magnetic intensity data displayed at 50 meter point spacing along line and 200m between lines. b) The point data gridded to make a Gocad© pseudo surface. c) Pseudo topography map where the magnetic value shown as the 'z' (all figures are from Gocad©).

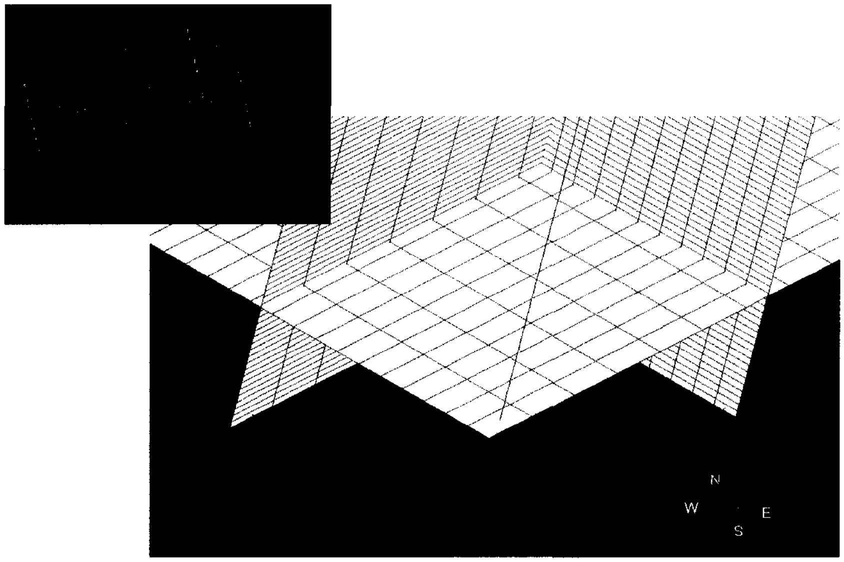

Figure 18. Voxets (3-D boxes) are used to capture data of interest in the study area. They are defined by U, V and W. In the case of the inset (upper left) the U (principle axis) is red and represents the X, the V is the green axis and represents the Y and the W is the blue axis and represents the Z. The larger image displays how the voxet can be divided by cells. The cell dimensions are created by the user according to how many intervals there will be across the three axises. A cell does not have to be equal width, depth and height.

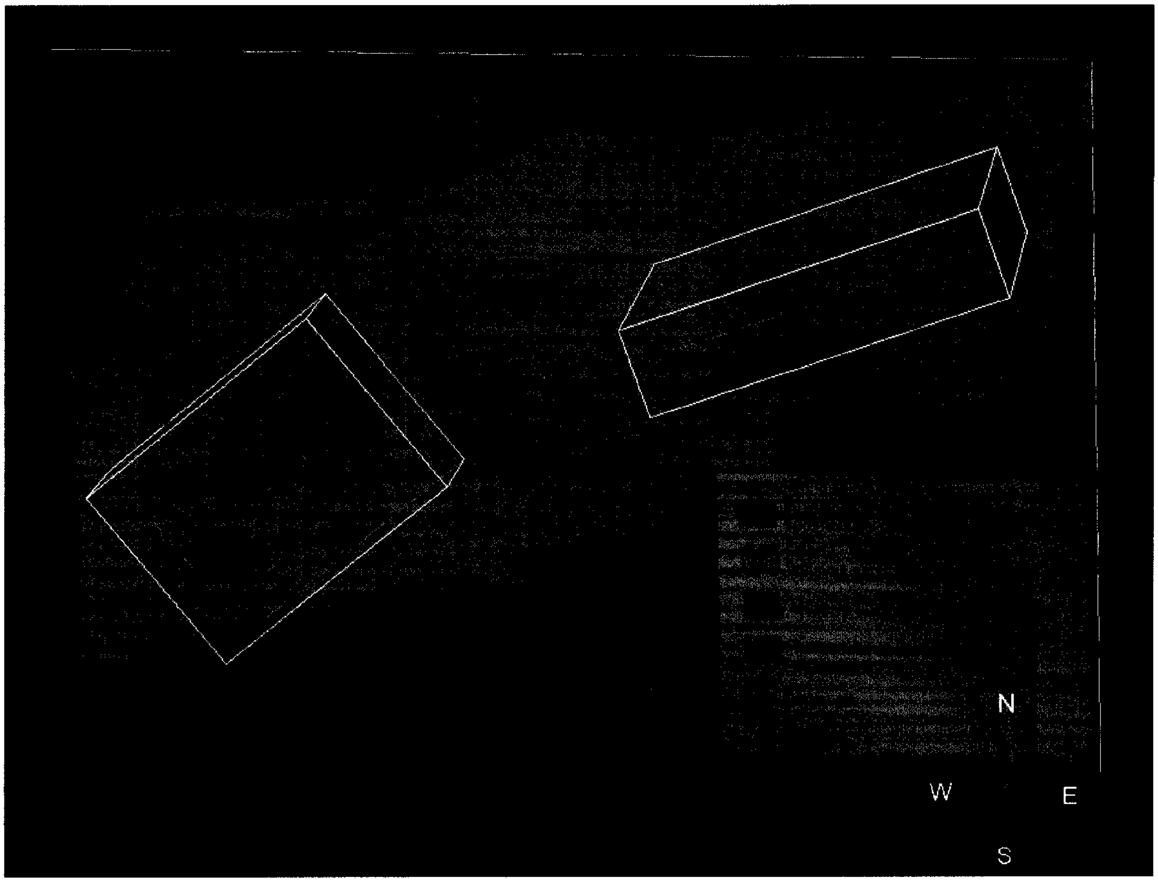

Figure 19. Figure 8b shown in Gocad© environment with voxets for B zone and ACD zone. These voxets are used to determine such parameters as distance from a cell in the voxet box to iron formation or massive sulfides.

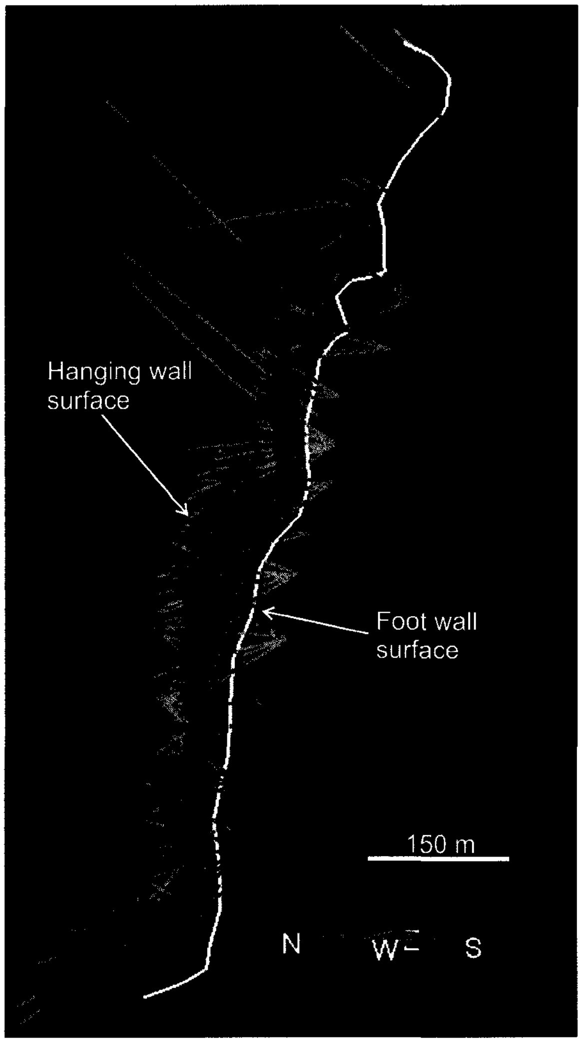

Figure 20. An example of how a hanging-wall and footwall surface can be interpreted by using the section tool called SPARSE© in Gocad©. The user can project data onto a section and then interpret surfaces between specific lithologies, such as in this example between the quartz±feldspar porphyry and massive sulfide (hanging wall: interpreted surface is purple) and the chloritic tuff and massive sulfide (foot wall: interpreted surface is yellow).

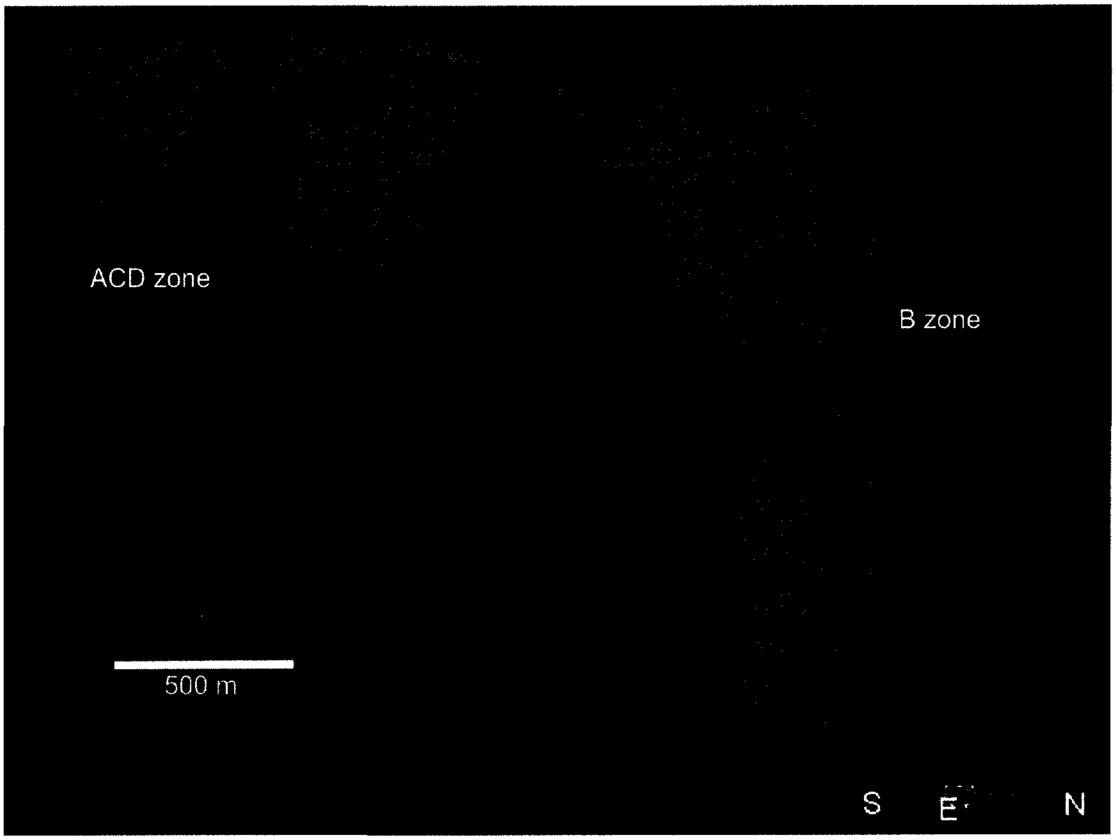

Figure 21. Looking from the East the more tabular nature of the B zone is clearly seen, where the ACD zone appears more pod shaped and does not extend as deep. Depth of the B zone displayed here is approximately 1100 m (scale bar applies to both vertical and horizontal).

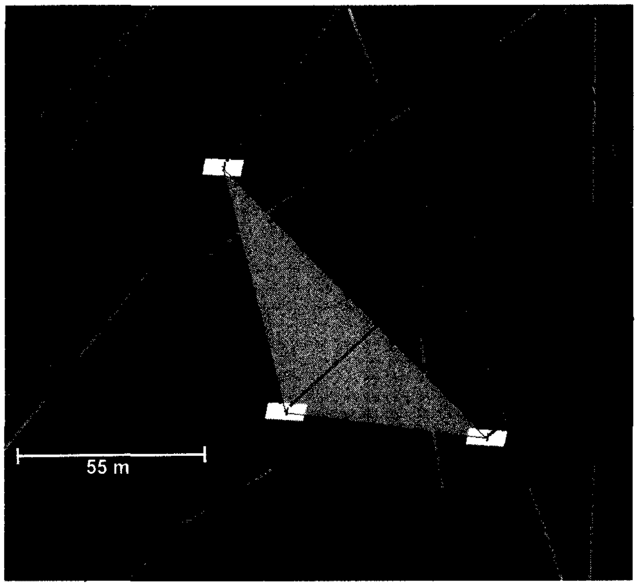

Figure 22. Three-dimensional view of drillcore data to show an example of the use of the model to establish contact relationships by displaying a section of drill core with colours representing different rock codes (red – massive sulfide, yellow – iron formation, orange – QFP and blue- chloritic tuff) points can be selected to represent a plane between lithologies. An example here is the boundary between massive sulfides and QFP. A polygon was used to connect three points and then a surface (shown in purple) interpreted to represent that plane. Dip markers (three yellow objects) can then be added to the points with the interpreted strike and dip of that surface.

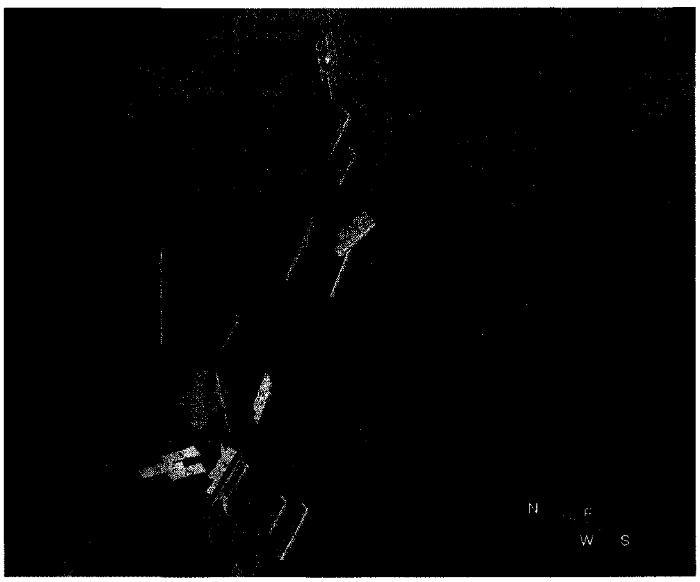

Figure 23. Three-dimensional cross section view looking east of the B zone. Dip markers created as in figure 23 are displayed with a transparent iso-surface of the B zone. The dip markers match the surface of the B zone iso-surface very well.

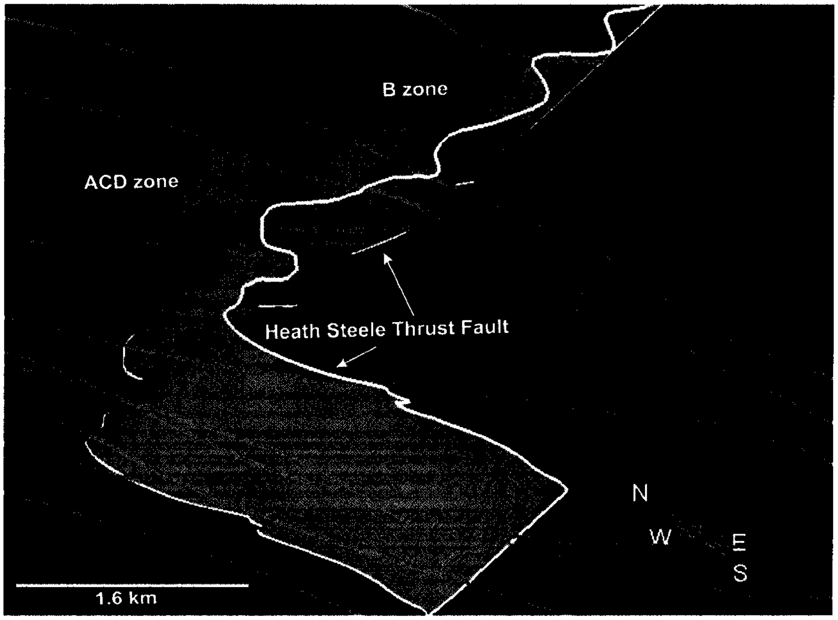

Figure 24. Three-dimensional perspective of the thrust fault taken from the regional geology map at a scale of 1:100 000 and extended to a depth of 1 kilometre below based on the strike and dip trend from the B and ACD zones. This procedure can be used to extrapolate data to view how a stratigraphic unit might be orientated at greater depths. Orange linear features displayed are regional faults.

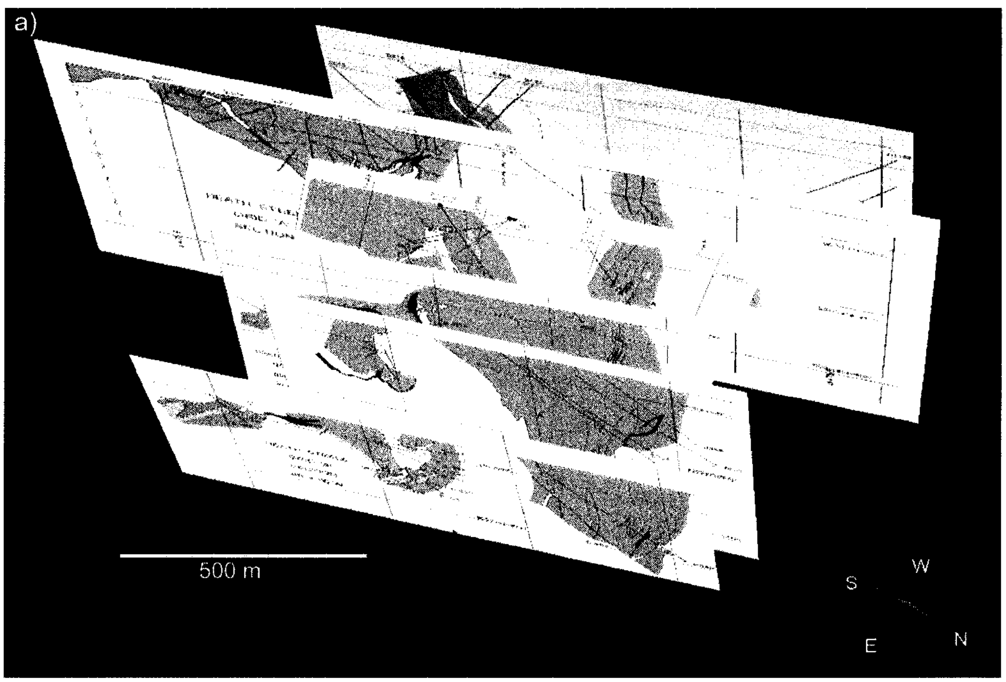

Figure 25. a) Six cross sections displayed as constructed by Noranda geologists. Quartz±feldspar porphyry is the orange unit and the chloritic tuff is the blue unit. It is difficult to join one feature such as the massive sulfides from one cross section to the next.

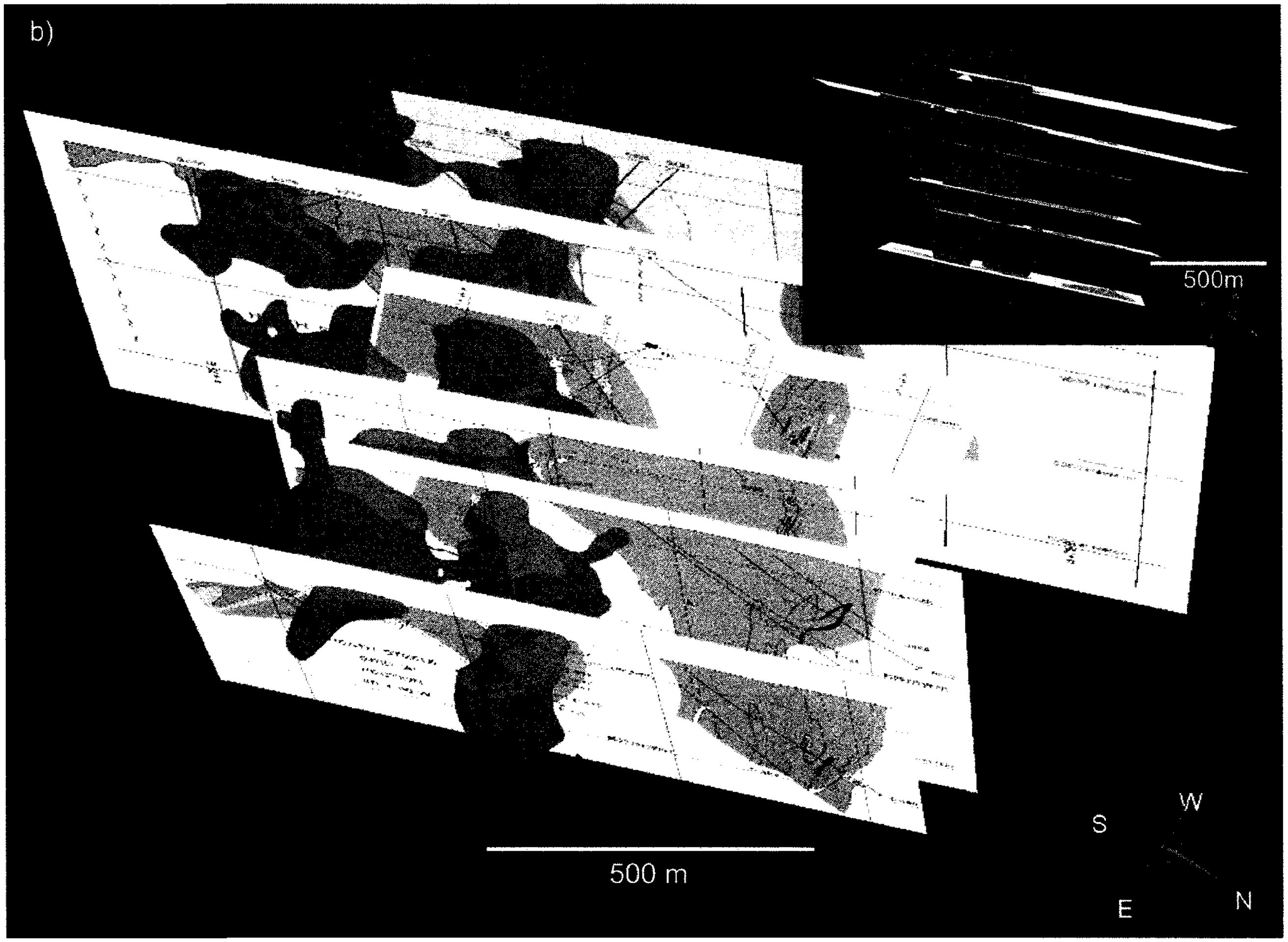

Figure 25. b) Correlations can be greatly assisted by modelling iso-surfaces from the drillhole data and associated dip information. Shown here is a modelled iso-surface of the massive sulfide body for the ACD zone (red semi-transparent body). The inset shows the same cross sections and iso-shell as plan view.

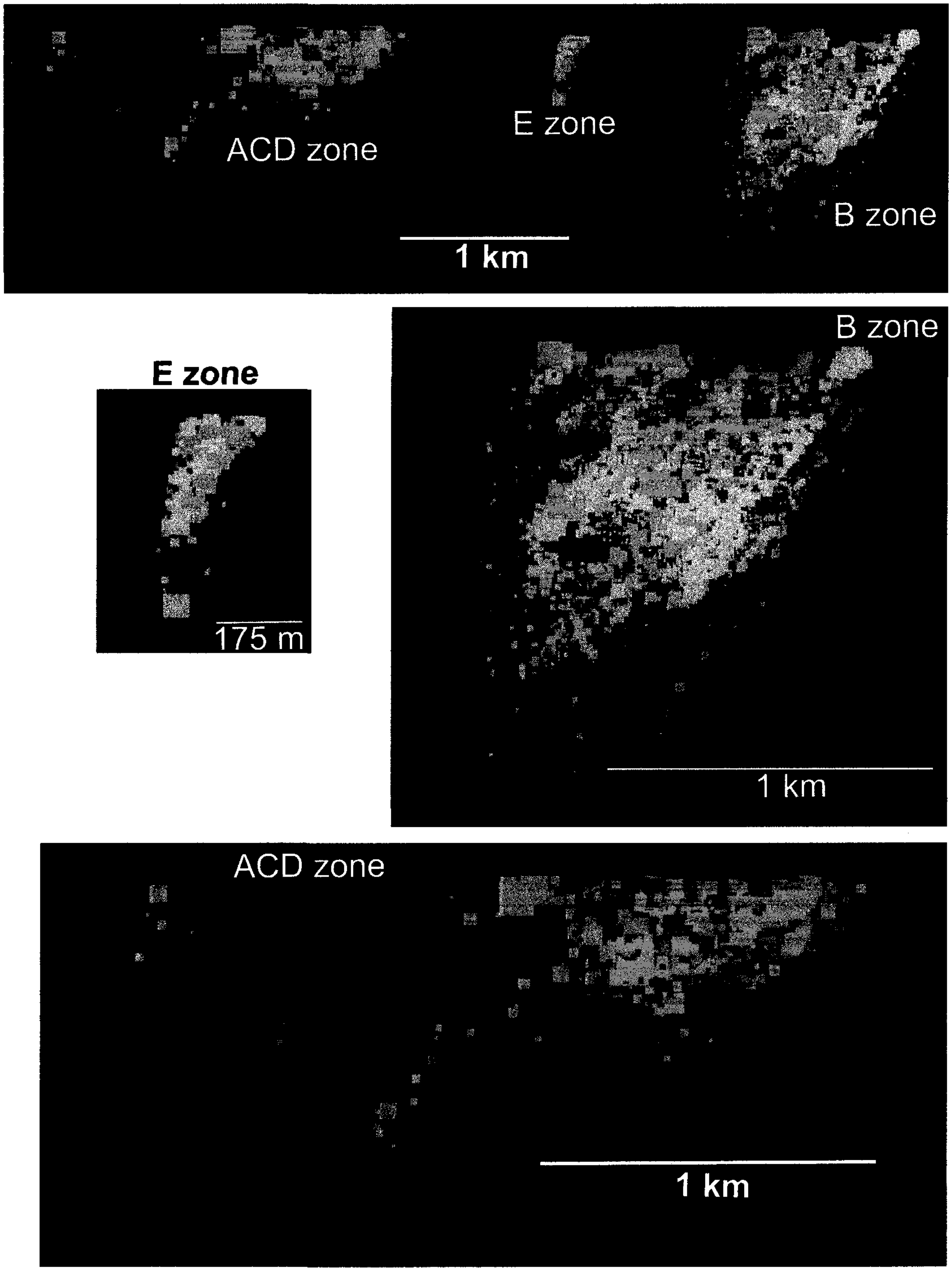

Figure 26. Illustration of grade distribution in the 3-D model of Heath Steele, view is from the south. Cu content (yellow) cut off at 0.5 %, Pb content (grey) cut off at 2.0%, and Zn content (brown) cut off at 5.5%. The size of the cube is dependant on the value, where the larger the number the larger the cube. Zoning of the Cu, Pb and Zn can be seen in both, but more obvious zones can be seen in B zone.

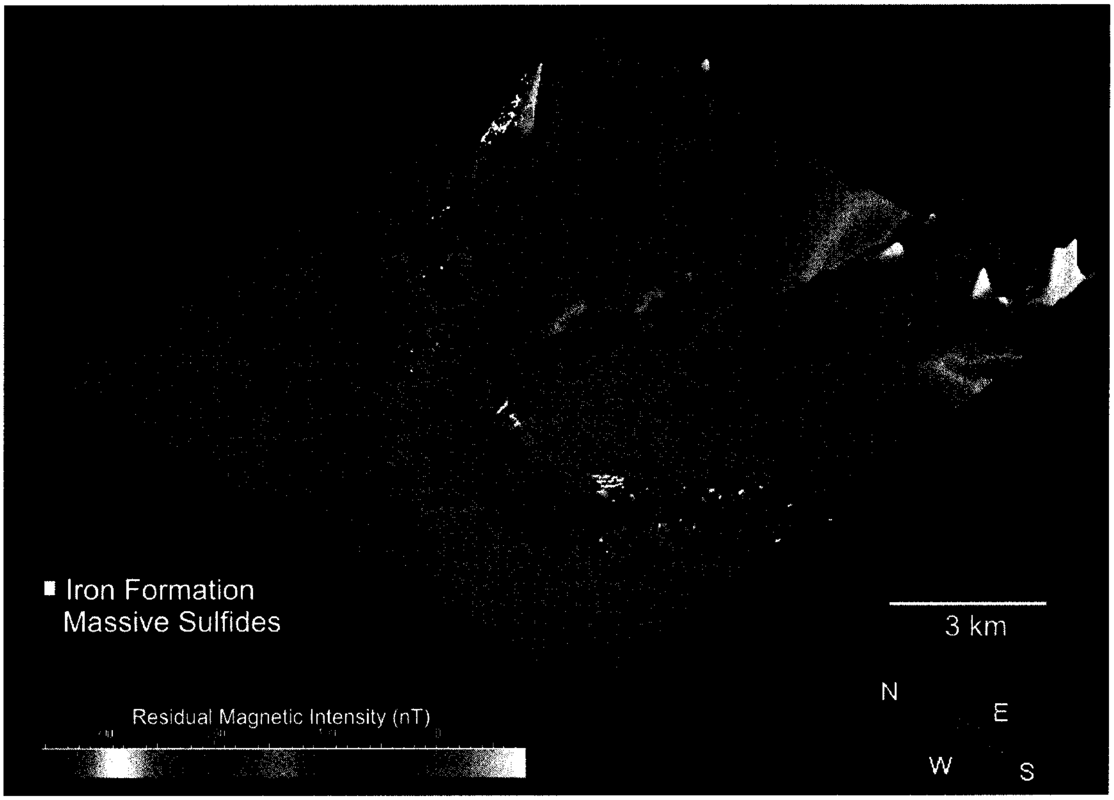

Figure 27. Gridded magnetic data with the massive sulfide (red dots) and iron formation (yellow dots). The magnetic values have been transposed to the Z value to show their amplitude. The massive sulfide and iron formation locations are projected above the surface to better show the correlation with the magnetic anomalies.

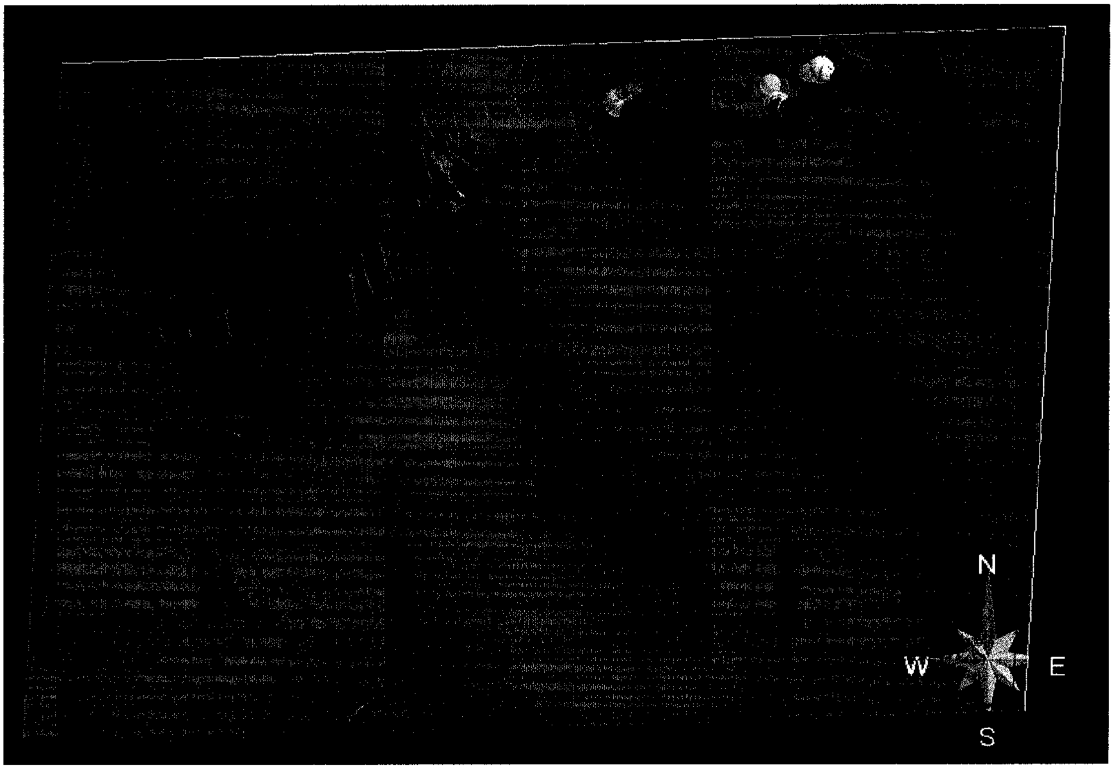

Figure 28. Actual figure from Peter (2003) used to display the hydrothermal sedimentary index values, shown here in the Gocad© 3-D environment. The drillcore pathways (red lines behind image) are projected in 3-D from the drill collar locations to depth seen behind the transparent image.

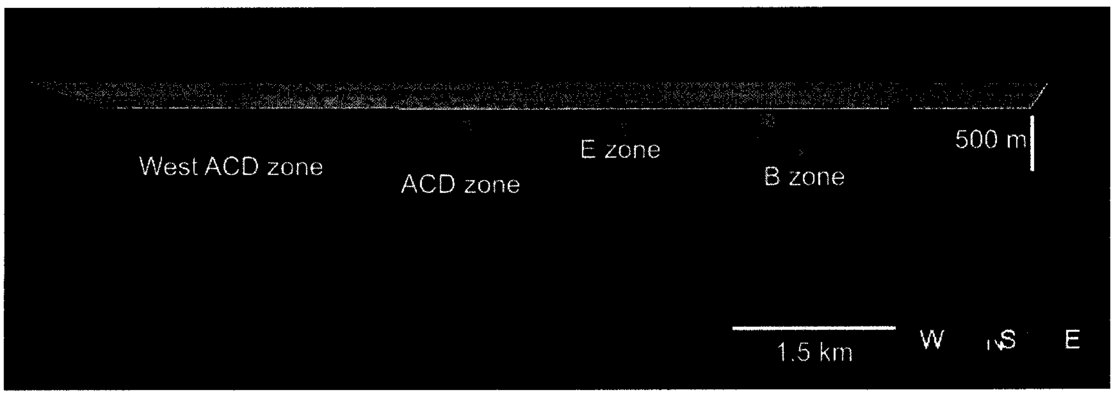

Figure 29. Same image as in figure 28, but tilted to see cross section view looking from the south to see the actual location of the hydrothermal sedimentary index values. All samples are shown here and shown as cubes where the size of the cube increases as the hydrothermal sedimentary index value increases. See Peter (2003) for explanation of Hydrothermal Sedimentary Index high and low values.

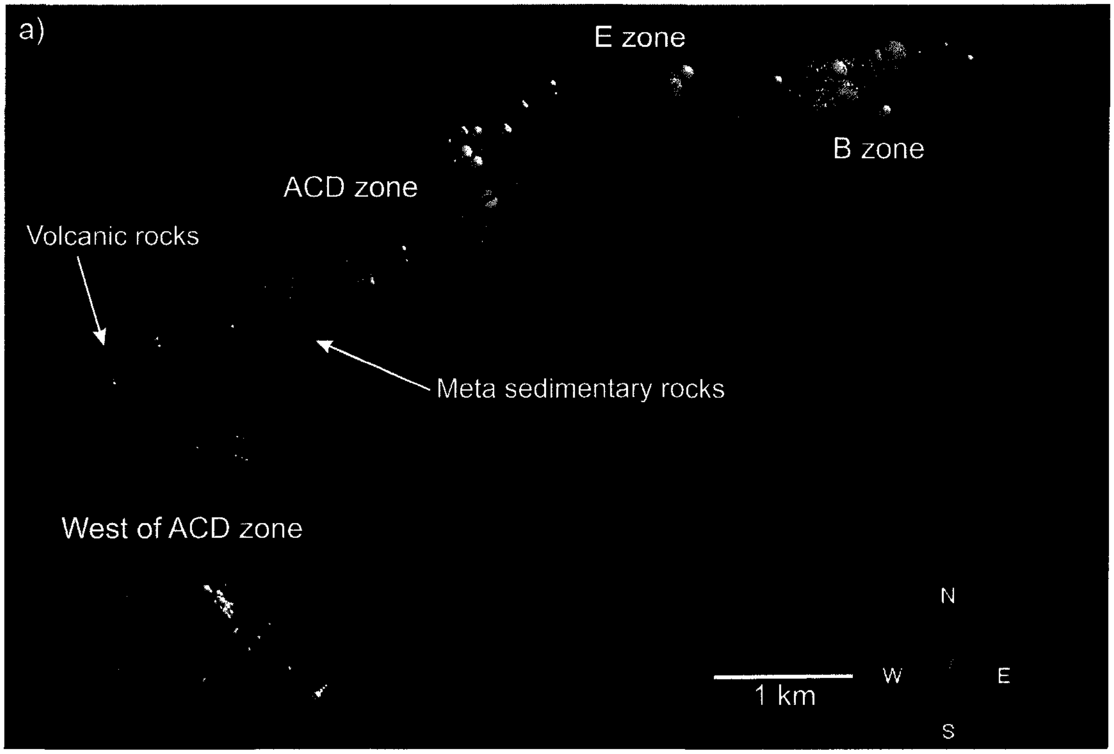

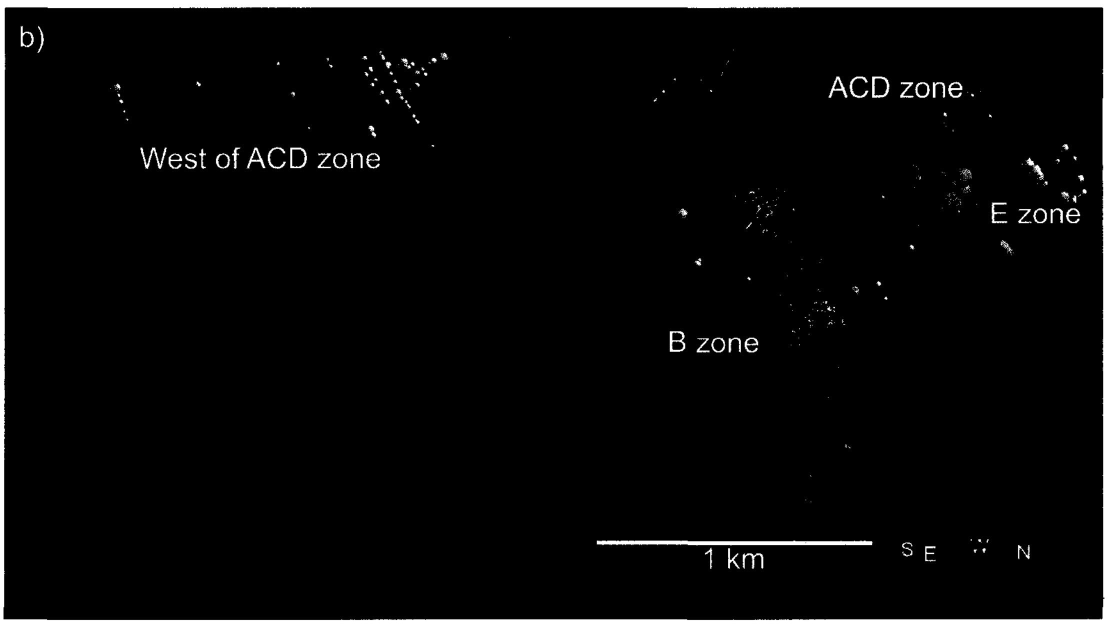

Figure 30. Hydrothermal Sedimentary Index values (see Peter, 2003 for further explanation of values) displayed with massive sulfide (red) and iron formation (yellow) drill core. a) shows a plane view of the Nepisiguit Falls Formations metasediments (transparent green) and volcanic (transparent yellow) rocks with the orebodies and hydrothermal sedimentary samples underneath. b) same data as in (a) but looking from east. The hydrothermal values are the white (low values, below 1) and blue (higher values, above 1) spheres where size is relative to their index value. From this perspective we can see the trend of the ore bodies and depth of hydrothermal index values.

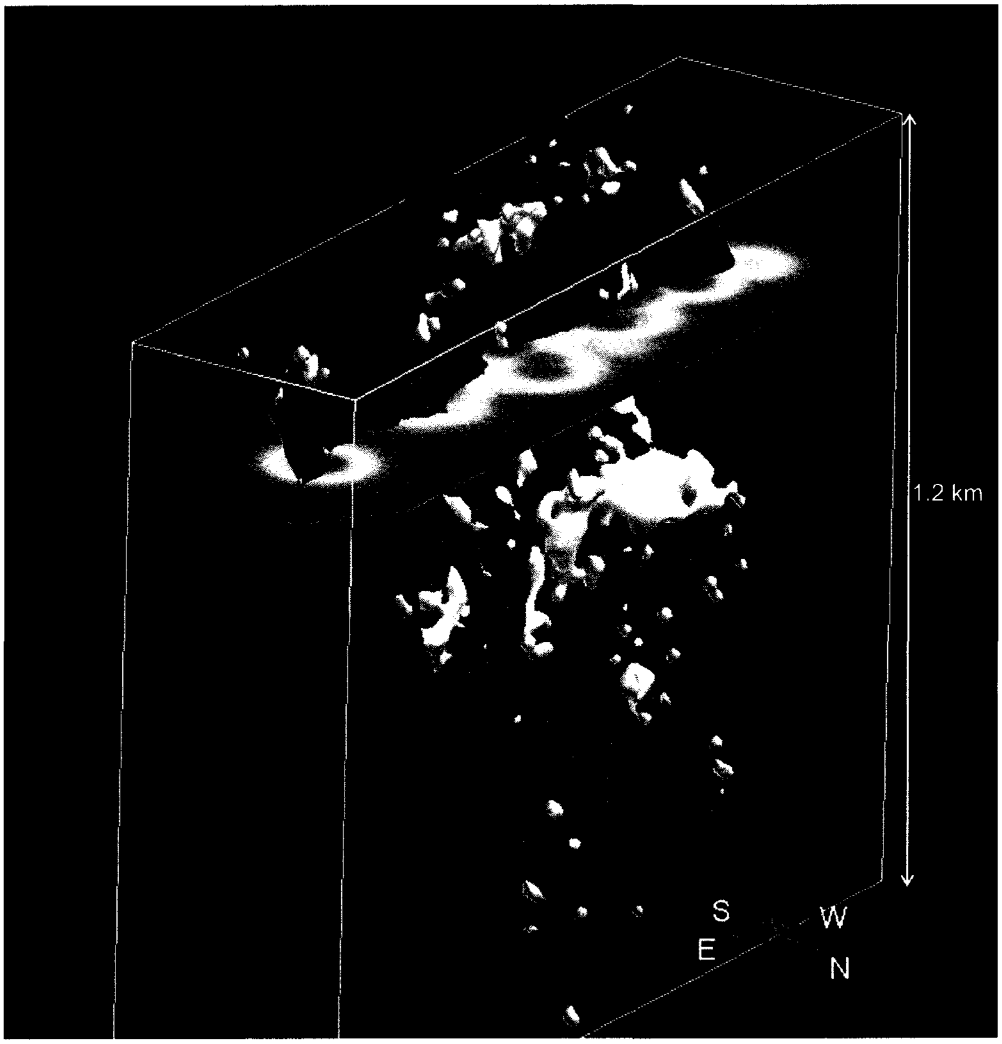

Figure 31. Modelled B zone massive sulfide surface (red) created by interpreting surface boundaries in SPARSE© cross sections. The iron formation (yellow) is modelled from iso-surfaces of distance from voxet to iron formation. The slice seen in the upper part of the voxet is a distance map of the massive sulfide to the iron formation (red is closest to iron formation then yellow, green and blue is the furthest). Even though there is association with the iron formation and massive sulfide, the record of the iron formation in the drill logs is not continuous.

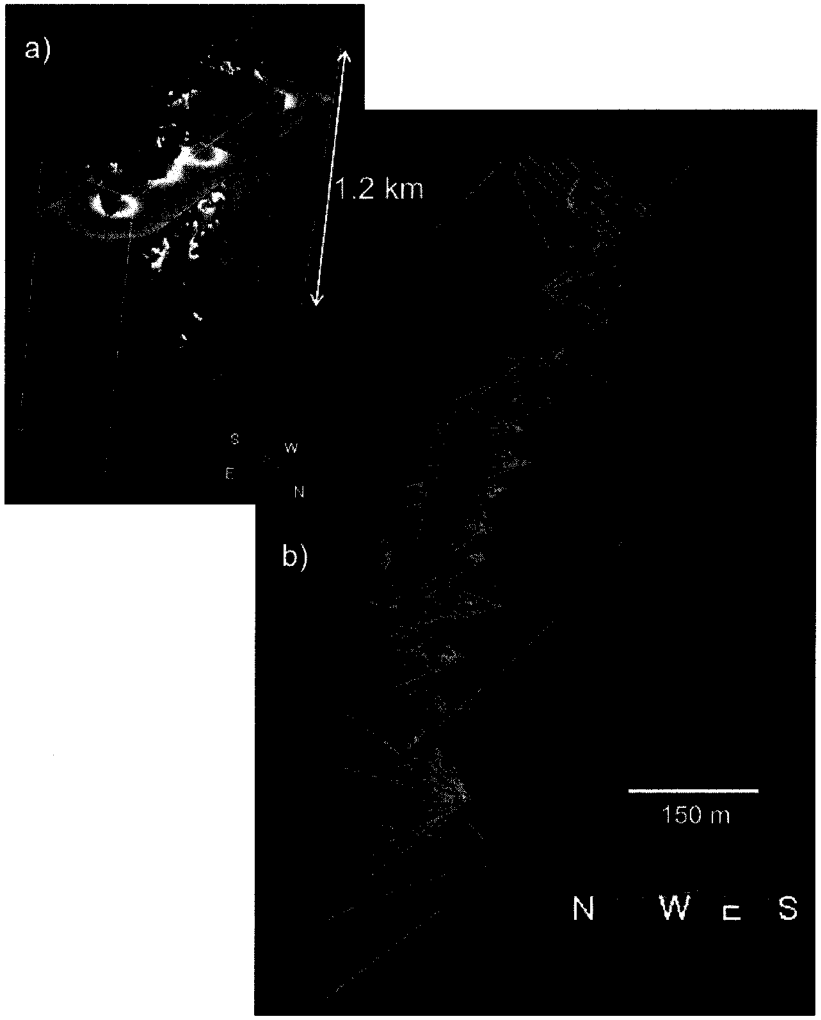

Figure 32. a) The grey slice with a green outline indicates location in the B zone orebody the 'SPARSE©' cross section is taken from for figure (b). b) Excellent examples are shown here in cross sections of the B zone where the hanging wall is well defined by quartz±feldspar porphyry (orange) and the foot wall defined is well defined by the chloritic tuff (blue). In the middle of this figure there is an indication of structure such as a possible fold in the massive sulfide body (red).

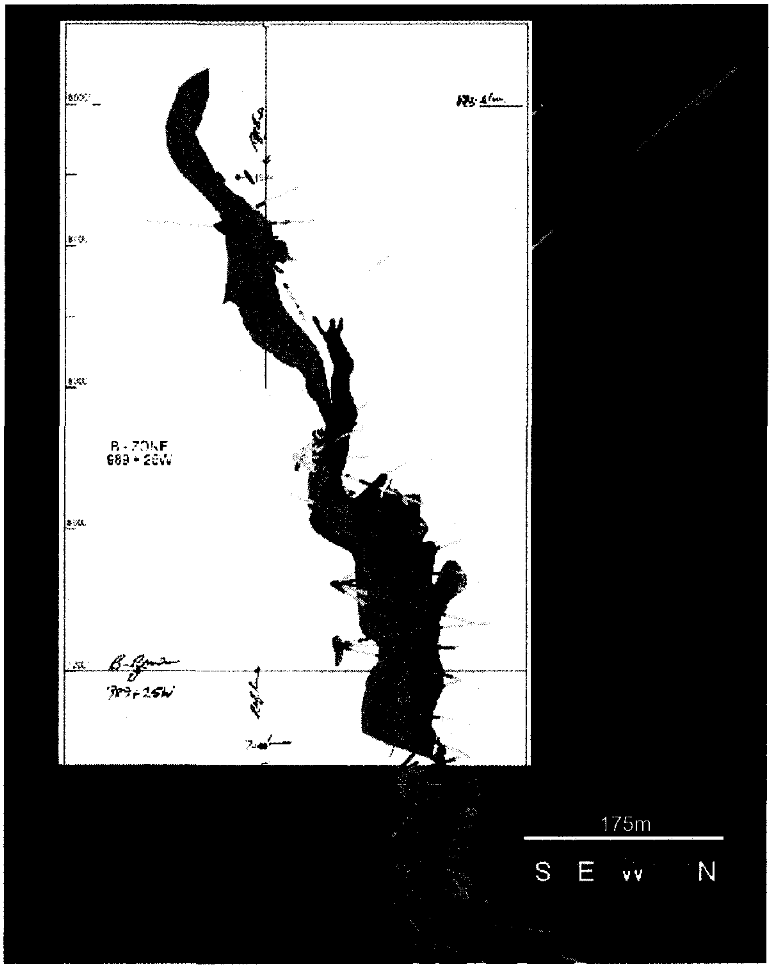

Figure 33. Cross sections interpreted from mine geologists were also brought into Gocad©. An example is shown with the drillcore data to highlight the complex structures the cross sections depict that cannot be substantiated by the drillcore data. Both the cross section image and the drillcore data are displayed in the Gocad© environment. Legend for the cross section according to mine geologists: red – massive sulfides, blue – waste sulfides, green – chloritic tuff, yellow – porphyry.

Appendix A:

Statistics of Gemcom Drillcore data used for Analysis and Model Construction of Heath Steele, New Brunswick.

ACD zone drillhole analysis			
	Subsurface	**Surface**	
Number of wells	1569	588	
Min depth of holes (meters)	3.05	15.54	
Max depth of holes (meters)	971.09	1210.06	
Average depth of holes (meters)	91.70	204.32	
Lithology intervals			
Min (meters)	0.03	0.01	
Max (meters)	234.70	388.62	
Average (meters)	9.02	10.52	
Count of intervals < 0.15 m	21	44	
Count of intervals	15871	512	
Assays intervals			
Min (meters)	0.06	0.03	
Max (meters)	32.77	12.01	
Average (meters)	1.89	1.38	
Count of intervals	24237	9921	
Assay statistics	Min	Max	Average
Cu	0	78.78	0.62
Pb	0	51.35	1.08
Zn	0	45.10	4.01

B zone drillhole analysis			
	Subsurface	Surface	
Number of wells	3233	455	
Min depth of holes (meters)	0.61	15.24	
Max depth of holes (meters)	966.52	1432.32	
Average depth of holes (meters)	94.89	192.85	
Lithology intervals			
Min (meters)	0.13	0.01	
Max (meters)	666.60	1185.06	
Average (meters)	11.63	11.28	
Count of intervals < 0.15 m	1	29	
Count of intervals	23513	7776	
Assays intervals			
Min (meters)	0.01	0	
Max (meters)	171.30	156.06	
Average (meters)	2.23	1.6	
Count of intervals	56535	6500	
Assay statistics	Min	Max	Average
Cu	0	51	0.91
Pb	0	30.84	1.23
Zn	0	56.8	3.09

West ACD zone drillhole analysis			
	Surface		
Number of wells	512		
Min depth of holes (meters)	64.62		
Max depth of holes (meters)	1165.85		
Average depth of holes (meters)	364.15		
Lithology intervals			
Min (meters)	0.01		
Max (meters)	374		
Average (meters)	13.14		
Count of intervals < 0.15 m	52		
Count of intervals	3780		
Assays intervals			
Min (meters)	0.03		
Max (meters)	12.19		
Average (meters)	1.23		
Count of intervals	1249		
Assay statistics	Min	Max	Average
Cu	0	18.8	0.352
Pb	0	14.86	0.301
Zn	0	18.75	0.72

Appendix B:

Conversion of Mine Grid data to New Brunswick NAD83
Stereographic Double Projection

Linear transformation equation from Mine Grid coordinates to New Brunswick NAD83 Double Stereographic coordinates:

$$x_{NB} = Ax_{MG} + By_{MG} + C$$
$$y_{NB} = Dx_{MG} + Ey_{MG} + F$$

Where: New Brunswick NAD83 Coordinates $= (x_{NB}, y_{NB})$ and
Mine Grid Coordinates $= (x_{MG}, y_{MG})$

NOTE: Mine Grid coordinates are in feet and New Brunswick NAD83 coordinates are in meters, therefore the mine coordinate input values MUST be first be converted to meters using a conversion factor; 1 foot = 0.3048 meters. Input numbers for thee calculations are given in Table 5.

matrix for x coordinates:

$$\delta = \begin{vmatrix} x_{MG1} & y_{MG1} & 1 \\ x_{MG2} & y_{MG2} & 1 \\ x_{MG3} & y_{MG3} & 1 \end{vmatrix} = 3.0305 \text{ x } 10^6$$

$$\delta_A = \begin{vmatrix} x_{NB1} & y_{MG1} & 1 \\ x_{NB2} & y_{MG2} & 1 \\ x_{NB3} & y_{MG3} & 1 \end{vmatrix} = 3.044 \text{ x } 10^6$$

$$\delta_B = \begin{vmatrix} x_{MG1} & x_{NB1} & 1 \\ x_{MG2} & x_{NB2} & 1 \\ x_{MG3} & x_{NB3} & 1 \end{vmatrix} = 3.4802 \text{ x } 10^4$$

$$\delta c = \begin{vmatrix} x_{MG1} & y_{MG1} & x_{NB1} \\ x_{MG2} & y_{MG2} & x_{NB2} \\ x_{MG3} & y_{MG3} & x_{NB3} \end{vmatrix} = 7.6448 \text{ x } 10^{12}$$

$$A = \frac{\delta_A}{\delta}, B = \frac{\delta_B}{\delta}, C = \frac{\delta_C}{\delta}$$

Where: A= 1.0044
B= 0.0115
C= 2522608

matrix for y coordinates:

$$\delta = \begin{vmatrix} x_{MG1} & y_{MG1} & 1 \\ x_{MG2} & y_{MG2} & 1 \\ x_{MG3} & y_{MG3} & 1 \end{vmatrix} = 3.0305 \text{ x } 10^6$$

$$\delta_D = \begin{vmatrix} y_{NB1} & y_{MG1} & 1 \\ y_{NB2} & y_{MG2} & 1 \\ y_{NB3} & y_{MG3} & 1 \end{vmatrix} = 1.7456 \text{ x } 10^3$$

$$\delta_E = \begin{vmatrix} x_{MG1} & y_{NB1} & 1 \\ x_{MG2} & y_{NB2} & 1 \\ x_{MG3} & y_{NB3} & 1 \end{vmatrix} = 3.0493 \text{ x } 10^6$$

$$\delta_F = \begin{vmatrix} x_{MG1} & y_{MG1} & y_{NB1} \\ x_{MG2} & y_{MG2} & y_{MB2} \\ x_{MG3} & y_{MG3} & y_{NB3} \end{vmatrix} = 2.2977 \text{ x } 10^{13}$$

$$D = \frac{\delta_D}{\delta}, E = \frac{\delta_E}{\delta}, F = \frac{\delta_F}{\delta}$$

Where: D= 5.76 x 10^{-4}
E= 1.0062
F= 7581916

Therefore the linear transformation equation to convert *Mine coordinates* to *New Brunswick NAD83* coordinates is:

$$x_{NB} = 1.0044 \cdot x_{MG} - 0.01155 \cdot y_{MG} + 2522608$$
$$y_{NB} = 0.000576 \cdot x_{MG} + 1.0062 \cdot y_{MG} + 7581916$$

Appendix C:

Sample of input files required for Gocad© to create drillcore path and populate it with properties

Table C1. Example of collar location file, bzone_header.csv

	A	B	C	D	E
1	HOLEID	LocationX_m	LocationY_m	LocationZ_m	Length_m
2	B10	723387.843	5242536.263	235.7	32.61
3	B1000	723778.002	5242783.743	-92.34	72.85
4	B1001	723777.925	5242783.805	-92.84	80.77
5	B1002	723775.978	5242780.696	-91.92	74.68
6	B1003	723977.537	5242838.628	102.85	43.59
7	B1004	723977.566	5242838.654	104.16	37.49
8	B1007	723963.69	5242832.437	102.93	68.58
9	B1009	723501.05	5242582.687	104.25	100.58
10	B1010	723562.864	5242730.71	61.86	55.47
11	B1011	723705.3	5242693.244	-91.65	117.35
12	B1012	723606.783	5242744.574	61.1	66.14
13	B1013	723785.735	5242737.078	-92.17	92.66
14	B1014	723785.942	5242737.014	-91.84	108.81
15	B1015	723823.669	5242816.369	-91.57	72.24
16	B1016	723705.3	5242693.226	-91.33	109.73
17	B1017	723692.028	5242684.334	-92.04	147.83
18	B1018	723692.05	5242684.233	-91.78	111.56
19	B1021	723719.46	5242695.559	-92.13	111.25
20	B1023	723778.198	5242757.437	-91.88	58.83
21	B1024	723789.138	5242730.231	-92.04	72.85
22	B1025	723788.194	5242729.319	-93.07	90.83
23	B1026	723671.641	5242665.675	183.27	128.02
24	B1027	723775.935	5242780.818	-92.62	80.16
25	B1028	723671.584	5242665.461	183.32	71.93
26	B1029	723787.897	5242729.381	-92.65	99.06
27	B1030	723788.168	5242729.375	-92.38	89.31
28	B1031	723853.55	5242728.394	222.76	74.98
29	B1032	723576.927	5242735.666	61.61	51.21
30	B1033	723547.49	5242725.216	62.55	66.45
31	B1034	723775.412	5242757.194	-92.56	85.34
32	B1035	723771.054	5242771.263	-92.31	90.53
33	B1036	723771.32	5242771.18	-92.04	75.29
34	B1037	723788.95	5242776.542	135.54	15.85
35	B1038	723789.962	5242774.426	135.54	14.94
36	B1039	723786.558	5242736.644	-91.94	91.44
37	B1040	723776.062	5242756.409	-91.66	84.43
38	B1041	723781.885	5242691.339	21.23	73.15
39	B1042	723775.234	5242694.633	20.88	141.12
40	B1043	723775.506	5242757.139	-91.99	82.6
41	B1044	723639.229	5242651.628	60.7	104.85
42	B1045	723640.136	5242962.659	61.23	73.21
43	B1046	723653.502	5242656.164	60.79	102.11
44	B1047	723776.563	5242780.66	-91.88	20.42

Table C2. Example of drill core pathway file, bzone_survey.csv

	A	B	C	D
1	HOLEID	Distance_m	AZIMUTH	DIP
2	B10	0	333.74	0
3	B1000	0	310	33.68
4	B1001	0	305.37	16.15
5	B1001	41.15	305.37	14.5
6	B1001	71.63	305.37	15
7	B1002	0	292.28	45.85
8	B1002	42.67	292.28	41
9	B1002	73.15	292.28	42
10	B1003	0	341.37	-5.81
11	B1004	0	343.73	32.51
12	B1007	0	343	-40
13	B1007	45.72	343	-44.5
14	B1009	0	283.65	6.6
15	B1009	45.72	283.65	9
16	B1009	73.15	283.65	9
17	B1010	0	162.2	-10.96
18	B1010	36.58	162.2	-12
19	B1011	0	342.62	17.43
20	B1011	45.72	342.62	14.5
21	B1011	97.54	342.62	13
22	B1012	0	165.02	-14.36
23	B1012	45.72	165.02	-17
24	B1013	0	289.32	25.81
25	B1013	30.48	289.32	26
26	B1013	82.3	289.32	26
27	B1014	0	289.15	41
28	B1014	45.72	289.15	39
29	B1014	102.11	289.15	39
30	B1015	0	343.2	39.06
31	B1015	48.77	343.2	32.5
32	B1016	0	343.63	29.41
33	B1016	45.72	343.63	28.5
34	B1016	92.96	343.63	25
35	B1017	0	343	8
36	B1017	45.72	343	0.5
37	B1017	99.06	343	3
38	B1017	138.68	343	3.5
39	B1018	0	342.7	20.73
40	B1018	45.72	342.7	15
41	B1018	106.68	342.7	14.5
42	B1021	0	342.38	21.4
43	B1021	45.72	341.38	16
44	B1021	111.25	341.38	15.5

Table C3. Example of geology file, b zone_rockcode.csv

	A	B	C	D
1	HOLEID	FROM	TO	RockCode
2	B10	0	0.3048	3
3	B10	0.3048	0.9144	1
4	B10	0.9144	9.144	3
5	B10	9.144	11.2776	1
6	B10	11.2776	13.4112	3
7	B10	13.4112	13.8684	1
8	B10	13.8684	15.0876	3
9	B10	15.0876	16.002	2
10	B10	16.002	18.7452	2
11	B10	18.7452	20.7264	1
12	B10	20.7264	23.3172	3
13	B10	23.3172	23.622	35
14	B10	23.622	24.0792	3
15	B10	24.0792	25.146	1
16	B10	25.146	26.3652	3
17	B10	26.3652	27.5844	3
18	B10	27.5844	28.194	1
19	B10	28.194	28.8036	4
20	B10	28.8036	32.6136	4
21	B1000	0	0.9144	0
22	B1000	0.9144	23.7744	1
23	B1000	23.7744	34.7472	6
24	B1000	34.7472	67.6656	3
25	B1000	67.6656	72.8472	4
26	B1001	0	0.9144	0
27	B1001	0.9144	21.9456	1
28	B1001	21.9456	36.8808	2
29	B1001	36.8808	78.6384	3
30	B1001	78.6384	80.772	4
31	B1002	0	0.9144	0
32	B1002	0.9144	27.1272	1
33	B1002	27.1272	31.3944	2
34	B1002	31.3944	39.9288	3
35	B1002	39.9288	40.5384	35
36	B1002	40.5384	66.7512	3
37	B1002	66.7512	74.0664	4
38	B1002	74.0664	74.676	3
39	B1003	0	0.9144	0
40	B1003	0.9144	19.5072	1
41	B1003	19.5072	28.0416	2
42	B1003	28.0416	32.6136	2
43	B1003	32.6136	41.148	3
44	B1003	41.148	42.9768	1
45	B1003	42.9768	43.5864	4

Table C4. Example of property file, b zone_assays.csv

	A	B	C	D	E	F
1	HOLEID	From	To	perCu	perPb	perZn
2	B10	0	0.3	2.75	0.11	0.81
3	B10	0.3	0.91	0.25	0.11	0.46
4	B10	0.91	2.44	1.9	0.11	0.6
5	B10	2.44	3.96	2.25	0.11	0.66
6	B10	3.96	5.39	2	0.11	0.51
7	B10	5.39	6.1	0.5	0.11	0.41
8	B10	6.1	7.62	0.6	0.11	0.41
9	B10	7.62	9.14	1	0.11	0.41
10	B10	10.36	11.28	0.9	0.11	0.2
11	B10	13.87	15.09	0.2	3.06	5.08
12	B10	15.09	16	0.3	0.27	1.93
13	B10	23.62	24.08	0.5	8.39	14.33
14	B10	25.15	26.37	0.65	2.2	5.03
15	B10	26.37	27.58	0.45	2.15	5.44
16	B10	27.58	28.19	0.3	1.67	4.06
17	B1000	34.75	35.97	0.26	0.2	0.19
18	B1000	35.97	36.58	0.26	0.2	0.19
19	B1000	36.58	39.62	0.08	1.08	2.8
20	B1000	39.62	42.98	0.08	0.28	6.41
21	B1000	42.98	46.33	0.75	1.65	10.37
22	B1000	46.33	49.38	0.26	2.6	10.28
23	B1000	49.38	52.43	2.97	0.26	0.32
24	B1000	52.43	55.78	1.05	0.24	0.25
25	B1000	55.78	59.13	2.04	0.3	0.23
26	B1000	59.13	60.96	0.59	0.46	6.14
27	B1000	60.96	64.31	1.02	0.26	1.86
28	B1000	64.31	67.67	1.14	0.5	0.99
29	B1001	36.88	40.23	0.87	0.23	1.11
30	B1001	40.23	43.59	0.06	1.61	5.01
31	B1001	43.59	46.94	0.1	1.23	2.41
32	B1001	46.94	50.29	0.87	0.77	3.06
33	B1001	50.29	52.73	0.7	2.48	12.13
34	B1001	52.73	55.47	0.7	2.12	11.92
35	B1001	55.47	58.22	1.3	0.83	1.44
36	B1001	58.22	60.96	0.36	0.34	0.24
37	B1001	60.96	63.4	1.65	0.4	2.19
38	B1001	63.4	66.45	1.3	0.28	1.05
39	B1001	66.45	69.19	0.92	0.4	1.3
40	B1001	69.19	72.24	0.17	0.5	1.82
41	B1001	72.24	75.29	0.08	0.48	0.39
42	B1001	75.29	78.64	0.07	3.31	11.16
43	B1002	31.39	33.53	0.82	0.43	2.07
44	B1002	33.53	35.66	0.66	0.25	2.45
45	B1002	35.66	38.1	0.15	0.19	1.4